

Inductive detection of Influence Operations via Graph Learning

Nicholas A. Gabriel¹, David A. Broniatowski², and Neil F. Johnson¹

¹Department of Physics, The George Washington University, Washington, DC 20052, USA

²Department of Engineering Management and Systems Engineering, The George Washington University, Washington, DC 20052, USA

May 25, 2023

Abstract

Influence operations are large-scale efforts to manipulate public opinion. The rapid detection and disruption of these operations is critical for healthy public discourse. Emergent AI technologies may enable novel operations which evade current detection methods and influence public discourse on social media with greater scale, reach, and specificity. New methods with inductive learning capacity will be needed to identify these novel operations before they indelibly alter public opinion and events. We develop an inductive learning framework which: 1) determines content- and graph-based indicators that are not specific to any operation; 2) uses graph learning to encode abstract signatures of coordinated manipulation; and 3) evaluates generalization capacity by training and testing models across operations originating from Russia, China, and Iran. We find that this framework enables strong cross-operation generalization while also revealing salient indicators—illustrating a generic approach which directly complements transductive methodologies, thereby enhancing detection coverage.

1 Introduction

Manipulation of public opinion by state-backed entities is an ongoing concern. Several influence operations (IO) campaigns intended to shape geopolitical discourse have been identified on various platforms—and particularly on social media [1–12]. For example, IO campaigns designed to promote fake news, advance nationalistic narratives, and exacerbate political tensions have been detected across social media platforms including Twitter [1, 5, 11, 12], Facebook [6–10, 13], Reddit [2, 14], and Gab [3, 15], among others. Identifying and disrupting such campaigns is an ongoing challenge, in large part because positive attribution of foreign influence is time consuming and does not easily scale within or across platforms. Additionally, the rapid development and adoption of generative AI may enable IO to automate behaviours previously achievable only by human actors, disguising activity and enabling novel strategies which have greater efficacy, scale, reach, and specificity. Most methods of detecting IO to this point have relied on identifying and indexing specific indicators of previous campaigns, making these methods inherently transductive. While such methods will continue to play an important role in detecting and constraining IO activity, identifying increasingly novel and sophisticated IO campaigns will require inductive methods which can generalize from previous observations. We present an inductive learning framework, depicted in Figure 5, that addresses this challenge by combining data censorship, graph learning, and feature attribution to identify models and indicators that can generalize across operations and across time.

Previous work in detecting influence operations using machine learning has successfully identified a variety of IO campaigns and activity. Broadly speaking, there have been two main approaches: *content-based* and *graph-based*. Some examples of content-based approaches include: Smith et al. [16], who used narratives derived from topic models to classify Twitter IO accounts in French and English speaking networks; and Alizadeh et al. [17] who used post text and URL information to classify Twitter posts as belonging to IO or not. Examples of graph-based approaches include: Monti et al. [18], who used graph networks (GNs) to classify URLs as fake news or not; Vargas et al. [19], who used graph data to classify IO accounts on Twitter which display coordinated behaviour; and Smith et al. [16], who used a network discovery algorithm followed by causal impact estimation to understand the role of individual accounts in propagating IO narratives.

A previously distinct line of research in cybersecurity, kill chain analysis [20–22], focuses on identifying and disrupting threat actors at each phase of their operation. This approach formalizes various sequences of tactics, techniques, and procedures (TTPs) which IO and other cybercrime operations use to achieve their objectives. In particular, online operations kill chains enable the development of technical indicators which are signatures of cybercrime operations at various phases. These indicators can be used to detect future operations, identify abstract

themes across campaigns, analyze trends, and compare TTPs across different operations and time periods.

These lines of research, as well as reports directly from social media companies, have elucidated a wide range of IO targets, objectives, strategies, and tactics. Many tactics involve the spread of malicious URLs [7], state-backed media, mis/disinformation [23], and particular narratives (e.g., pro-Russian narratives surrounding the Ukrainian war [6, 8, 9]); other tactics include near-simultaneous link sharing [24], troll farming [7], mass promotion of particular narratives [6, 7, 16], mass reporting of accounts and content [7, 9], and mass spamming or “brigading” of specific pages, posts, and users [7]. Identifying these tactics has enabled well-resourced social media companies such as Twitter, Meta, and Google to automate the detection of new campaigns that reuse TTPs on their respective platforms. This automation has in turn enabled rapid detection and response to coordinated IO activity.

Automated detection has greatly constrained the preferred tactics available to IO on relatively well-regulated platforms such as Facebook and Twitter. For example, networks of coordinated and near-simultaneous link sharing (<1 min. apart) are now quickly and routinely removed from these platforms [7–11, 25]. However, this conspicuous behaviour persists as an IO tactic due to the fact that social media ranking algorithms up-rank content with higher engagement, with immediate engagement having an outsized effect on relative ranking and ultimate reach of content [26]. Hence, to artificially amplify specific narratives during critical periods, IO preferentially coordinate on very short timescales, even at risk of being detected. So while near-simultaneous coordination may be largely curtailed by platforms or even abandoned by IO in the future, coordination on short timescales is expected to continue. For particularly sophisticated IO networks, one would expect that future coordination patterns would mimic that of authentic users.

<div> <div>coordination time</div> <div>fake account type</div> </div>	near-simultaneous (< 1 min.)	quasi-authentic (< 100 min.)
spam accounts	<i>immediately detectable</i>	<i>detectable</i>
persona building	<i>detectable</i>	<i>currently undetectable</i>

↑ increased cost
↓

← decreased efficacy →

Figure 1. Current landscape of automated detection on mainstream social platforms. Advances in automated detection will push influence operations towards less effective methods of coordination and more costly approaches to fake account creation. In turn, influence operations may be able to compensate by augmenting existing capabilities with emergent AI systems.

Fake account detection [7, 9–11] has also greatly improved. In response, IO have tried to obviate detection by crafting realistic profiles that mimic authentic users in a process called *persona building*. The process of persona building has presumably been a manual effort to this point, as smaller numbers of these meticulously crafted fake accounts are observed as part of any IO compared to the much larger numbers of less sophisticated “spam” accounts

(though part of this discrepancy may be a survivorship bias). A common approach to persona building is to mimic existing accounts that promote narratives favorable to the IO objective, such as inflammatory political content promoted by Russian and Iranian IO campaigns leading up to the 2016 and 2020 U.S. presidential elections [11, 25]. This process of mimicry requires significant investment of human effort, as this approach requires the generation of novel content such as text and images. However, it is not difficult to imagine that in the near future a single IO operative could automate the persona building process using novel AI tools to farm a large number of fake accounts. Indeed the use of GAN produced profile pictures [10, 20] and deep fakes [27] has been reported. While the automated detection of near-simultaneous coordination and fake accounts will push campaigns towards less efficacious and more costly approaches (Figure 1), they may be able to compensate with greater scalability, novelty, and specificity enabled by AI.

While mainstream platforms have the resources and desire to improve regulation, alternative platforms are less equipped, and possibly unwilling, to follow suit. Exploiting this situation, the Russian origin Secondary Infektion campaign from 2014-2020 made use of over 300 platforms including WordPress, BlogSpot, Quora, Reddit, and LiveJournal to circulate fake news and seed fabricated primary sources [28]. A subsequent Russian campaign from 2020-2022 (likely a continuation of the same operation) targeted 35 alternative platforms that intentionally have little or no regulation such as Gab, Gettr, Parler, and Truth Social [23]. While all of these platforms combined have a smaller audience than most mainstream platforms, they demonstrate continued trends of IO in microtargeting specific audiences and diversifying channels of influence. Countering these trends will require methods of detection that can identify operations across platforms, as well as generalize previous observations on mainstream platforms to newly targeted platforms. Additionally, while mainstream platforms have thus far been proactive in identifying and removing inauthentic actors, it is unclear to what extent this will continue to be true.

Even in light of these trends, continuing to identify and index TTPs for transductive detection will still be paramount to constrain future IO. In other words, the foundation of IO detection will continue to be transductive—or based on specific, previously observed indicators. Transductive approaches will continue to be effective in constraining IO for two main reasons: 1) operations can only develop new TTPs so quickly; 2) previously indexed TTPs often represent the preferred tactics of IO, which they may be slow to abandon. In order to continue shaping public discourse in the near term, one can then expect continued reuse of TTPs, even if these are largely ineffective on mainstream platforms. In the long term, however, one can expect IO to develop novel tactics that avoid detection and reach larger segments of online users. On one hand, this means that future IO will likely have less impact per action (post, like, share, etc.) since they cannot maximally exploit the platforms in which they are embedded. On the other hand, AI systems such as StyleGAN2 [29], DeepFaceLab [30], GPT [31], and DALL-E [32] may allow IO to more easily craft realistic profiles and content, thereby enabling novel campaigns that employ previously costly tactics at greater scale. In such cases, it is unclear how effective transductive methods will be, if at all. Hence, developing inductive methods of detection will be necessary to proactively identify and disrupt novel campaigns which can consequentially alter public opinion in a matter of days (e.g., in the days leading up to an election [11, 25]). To this end, we observe two fundamental techniques that IO use when manipulating public opinion:

- (I) linking to off-platform websites that are considered credible by the target audience and/or possessing decreased regulation;
- (II) coordinated promotion of content supporting specific narratives.

Arguably, IO can have little impact on public opinion without employing these techniques in some form. We use this observation to design (I) content-based and (II) graph-based indicators which are general enough to identify novel campaigns from previous campaigns, and use graph representation learning to encode abstract signatures of coordination from these indicators. In particular, we determine indicators that are not specific to any particular IO campaign by explicitly censoring previously identified content- and graph-based technical indicators. We call indicators resulting from this type of censorship *generalized indicators*, since they will be common across both IO campaigns and authentic users, and also across platforms.

We investigate how specific choices of generalized indicators and graph learning techniques can identify inauthentic actors across IO campaigns, thereby developing a framework that directly complements the transductive methodologies established in previous work. In doing so, we note the correspondence between the generalized indicators used here and previously used technical indicators:

feature type	technical indicator [16, 17, 19, 20, 24]	generalized indicator
content-based	political and news domains; URLs containing malware, propaganda, and fake news	censored domains
graph-based	graph size, betweenness, clustering	censored graph learning
coordination	near-simultaneous (<1 min.)	quasi-authentic (<100 min.)

Table 1. Correspondence between previously effective technical indicators and generalized alternatives.

Furthermore, we investigate three specific advances of previous approaches:

- (1) Identification of content-based and graph-based indicators which enable cross-operation generalization;
- (2) Utilization of graph learning to encode abstract signatures of coordination, thereby automating graph-based feature engineering and inference;
- (3) Investigation of a broad coordination window, moving from near-simultaneous (<1 min.) to quasi-authentic (<100 min.) interarrival times.

2 Results

Following the framework presented in Figure 5, we assess the extent to which specific machine learning models and generalized indicators can identify IO accounts across campaigns, both intra-operation and inter-operation (results shown in Table 2). For this purpose, we select six IO campaigns (Figure 2) belonging to three coordinated operations: Russia, China, and Iran; and a comprehensive baseline described in the next section. We analyze intra- and inter-campaign co-URL statistics in Figure 4, demonstrating operation specific trends and the independence of the three operations chosen. In Table 3, we determine which indicators enable cross-campaign generalization using an axiomatic attribution method, integrated gradients [33].

Train/Validate:

origin	removal date	accounts	target
Russia	Oct. 2018	3378	U.S./Rus.
Iran	June 2019	1448	Varied [‡]
China	Aug. 2019	472	Hong Kong
total		5298	

Test:

origin	removal date	accounts	target
Russia	May 2020	1059	U.S./Rus.
Iran	Feb. 2021	179	U.S.
China	May 2020	4201	Varied [¶]
total		5439	

Baseline:

origin	removal date	accounts	category
U.S./U.K.	-	2681	Political
-	-	5983	Random
Varied [§]	-	1129	Top RT
total		9793	

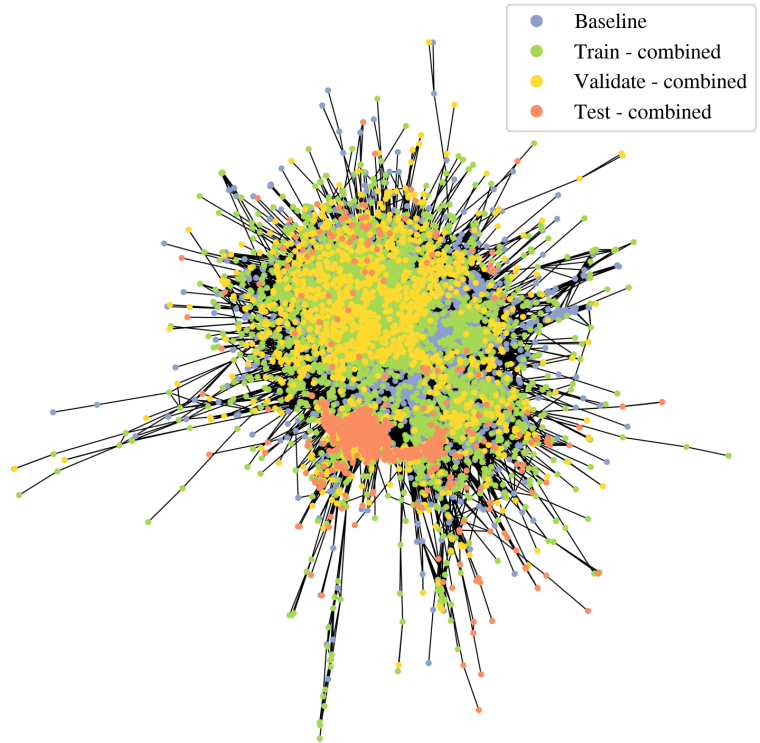


Figure 2. Composition of training, validation, and test and baseline sets.

[‡] target audiences includes the U.S., Latin America, Saudia Arabia, Israel, Indonesia.

[¶] target audiences includes the U.S., China, and Russia.

[§] account origins include U.S., Russia, and China

2.1 Model and Indicator Evaluation

We evaluate the effectiveness of several machine learning models—Logistic Regression (LR), Random Forest (RF), Multilayer Perceptron (MLP), Graph Convolutional Network (GCN), deep Message Passing Neural Network (MP-GCN), and shallow Message Passing Neural Network (MP-GCN(s))—on node classification tasks comprising: 10737 influence operation accounts reported by Twitter between 2018 and 2021; and 9793 baseline Twitter accounts not known to be part of any influence operation. The IO accounts were reported in several releases between October 2018 and February 2021, which we split as in Figure 2 to simulate a prediction task on unseen data. The baseline includes accounts which directly impact public discourse (journalists, media outlets, writers, and academics), random accounts, and accounts highly retweeted by the IO training set. Our goal is to differentiate IO accounts versus this baseline using a set of generalized indicators, as well as determine the optimal graph encoding (G.E.) for each model (i.e. which of **node2vec**, **Laplacian Eigenmaps**, **Random Walk Positional Encoding**, and **Network Features** to include).

In order to assess the generalization capacity of particular model and indicator choices, we formulate two tasks. The first is intra-operation classification (**A** in Table 2), where we train on a campaign of a particular operation (Russia, China, or Iran) and test on a later identified campaign of same operation. The second task is inter-operation classification (**B** in Table 2), where we train on all operations *except* the test operation. For the three campaigns in the training/validation set and the test set, this implies three subtasks for **A** and **B**. To enable comparison between the two sets of subtasks, we sample the validation and test sets for each respective subtask identically (e.g., the results of task **A1** and **B1** can be compared directly). This allows us to assess how well each model can generalize from independent operations based on any changes in performance from tasks **A1**, **A2**, and **A3** to tasks **B1**, **B2**, and **B3**, respectively.

We evaluate the effect of varying the content-based feature set both in terms of stringency (γ_{\max}) and minimum prevalence (k_{top}) on model performance in Figure 3. We choose MLP with all graph encodings (G.E. = ††††) as a representative model since it consistently performed well across all subtasks. The effect of increasing k_{top} improves model performance on all metrics in a nearly monotonic manner, ostensibly reaching saturation around $k_{\text{top}} = 2000$. The effect of varying the maximum frequency ratio (γ_{\max}) has a more nuanced effect on performance, but a fairly stringent value of $\gamma_{\max} \in \{0.43, 0.67\}$ appears to produce greater generalization than smaller or larger values, with increases beyond $\gamma_{\max} = 0.67$ producing a nearly monotonic decrease in performance for F1(val/test), but not for AUC.

(A): Combined, intra-operation					(B): Combined, inter-operation				
model	F1(val.) [‡]	F1(test)	AUC(test)	G.E.	model	F1(val.)	F1(test)	AUC(test)	G.E.
LR	92.92	84.94	85.23	*†††	LR	82.97	76.92	77.64	*†††
RF	97.50	86.58	86.90	****	RF	82.36	81.06	81.52	****
MLP	95.96	91.13	94.68	††††	MLP	92.04	89.92	96.59	††††
GCN	95.33	91.71	91.79	††††	GCN	86.39	91.25	93.92	††††
MP-GCN(s)	95.55	91.02	94.44	††††	MP-GCN(s)	91.65	88.05	96.28	††††
MP-GCN	95.49	90.64	93.01	††††	MP-GCN	92.40	88.06	96.05	††††

(A1): Rus(18) → Rus(18) / Rus(20)					(B1): Chn(19) + Iran(19) → Rus(18) / Rus(20)				
$N_{\text{train}}^{(y=1)} = 2702 \rightarrow N_{\text{val./test}}^{(y=1)} = 676/1059$					$N_{\text{train}}^{(y=1)} = 1920 \rightarrow N_{\text{val./test}}^{(y=1)} = 676/1059$				
model	F1(val.) [‡]	F1(test)	AUC(test)	G.E.	model	F1(val.)	F1(test)	AUC(test)	G.E.
LR	96.25	90.27	90.45	††††	LR	91.93	89.91	90.11	*†††
RF	99.09	91.82	92.95	††††	RF	83.50	86.46	86.71	****
MLP	97.27	91.90	96.72	††††	MLP	90.11	90.48	96.77	††††
GCN	94.80	90.10	93.83	††††	GCN	84.64	92.22	93.63	††††
MP-GCN(s)	96.29	92.80	95.46	††††	MP-GCN(s)	86.12	93.21	94.43	††††
MP-GCN	96.36	92.84	95.41	††††	MP-GCN	86.15	93.44	94.51	††††

(A2): Chn(19) → Chn(19) / Chn(20)					(B2): Rus(18) + Iran(19) → Chn(19) / Chn(20)				
$N_{\text{train}}^{(y=1)} = 377 \rightarrow N_{\text{val./test}}^{(y=1)} = 95/4201$					$N_{\text{train}}^{(y=1)} = 4826 \rightarrow N_{\text{val./test}}^{(y=1)} = 95/4201$				
model	F1(val.) [‡]	F1(test)	AUC(test)	G.E.	model	F1(val.)	F1(test)	AUC(test)	G.E.
LR	94.54	88.08	88.30	*†††	LR	89.23	82.66	83.08	††††
RF	97.06	91.75	91.87	****	RF	82.31	93.47	93.54	****
MLP	95.44	92.63	93.70	††††	MLP	91.52	94.63	97.82	†**†
GCN	95.40	92.83	89.26	††††	GCN	90.40	94.41	97.51	††††
MP-GCN(s)	95.04	93.57	92.56	††††	MP-GCN(s)	92.10	94.16	97.38	††††
MP-GCN	95.26	93.33	90.15	††††	MP-GCN	91.79	94.78	97.29	††††

(A3): Iran(19) → Iran(19) / Iran(21)					(B3): Chn(19) + Rus(18) → Iran(19) / Iran(21)				
$N_{\text{train}}^{(y=1)} = 1158 \rightarrow N_{\text{val./test}}^{(y=1)} = 290/179$					$N_{\text{train}}^{(y=1)} = 3850 \rightarrow N_{\text{val./test}}^{(y=1)} = 290/179$				
model	F1(val.) [‡]	F1(test)	AUC(test)	G.E.	model	F1(val.)	F1(test)	AUC(test)	G.E.
LR	88.36	77.60	78.01	*†††	LR	73.36	71.36	72.56	****
RF	96.38	77.06	77.64	****	RF	71.94	75.01	75.61	****
MLP	95.21	88.95	93.69	††††	MLP	89.57	86.58	98.41	††††
GCN	95.80	92.26	92.40	††††	GCN	75.62	87.39	92.05	††††
MP-GCN(s)	95.33	86.97	95.35	††††	MP-GCN(s)	87.85	83.67	96.15	††††
MP-GCN	94.87	86.13	93.61	††††	MP-GCN	90.65	84.01	97.37	††††

Table 2. Top: Aggregated intra-operation (A) and inter-operation (B) results; F1 and ROC-AUC scores are the harmonic mean of the individual subtasks shown in the bottom six tables; G.E. is the median value of subtasks. Bottom: Individual subtask results for intra-operation (A1, A2, and A3) and cross-operation (B1, B2, and B3) classification. We note that the validation and test sets in the intra-operation and cross-operation subtasks are sampled identically, and hence can be compared. Each graph encoding (G.E.) denotes the absence (*) or presence (†) of **node2vec**, **Laplacian Eigenmaps**, **Random Walk Positional Encoding**, and **Network Features** determined from a censored graph. Each model is trained with $\gamma_{\max} = 0.54$ and $k_{\text{top}} = 2500$ per Figure 3. ‡In sample.

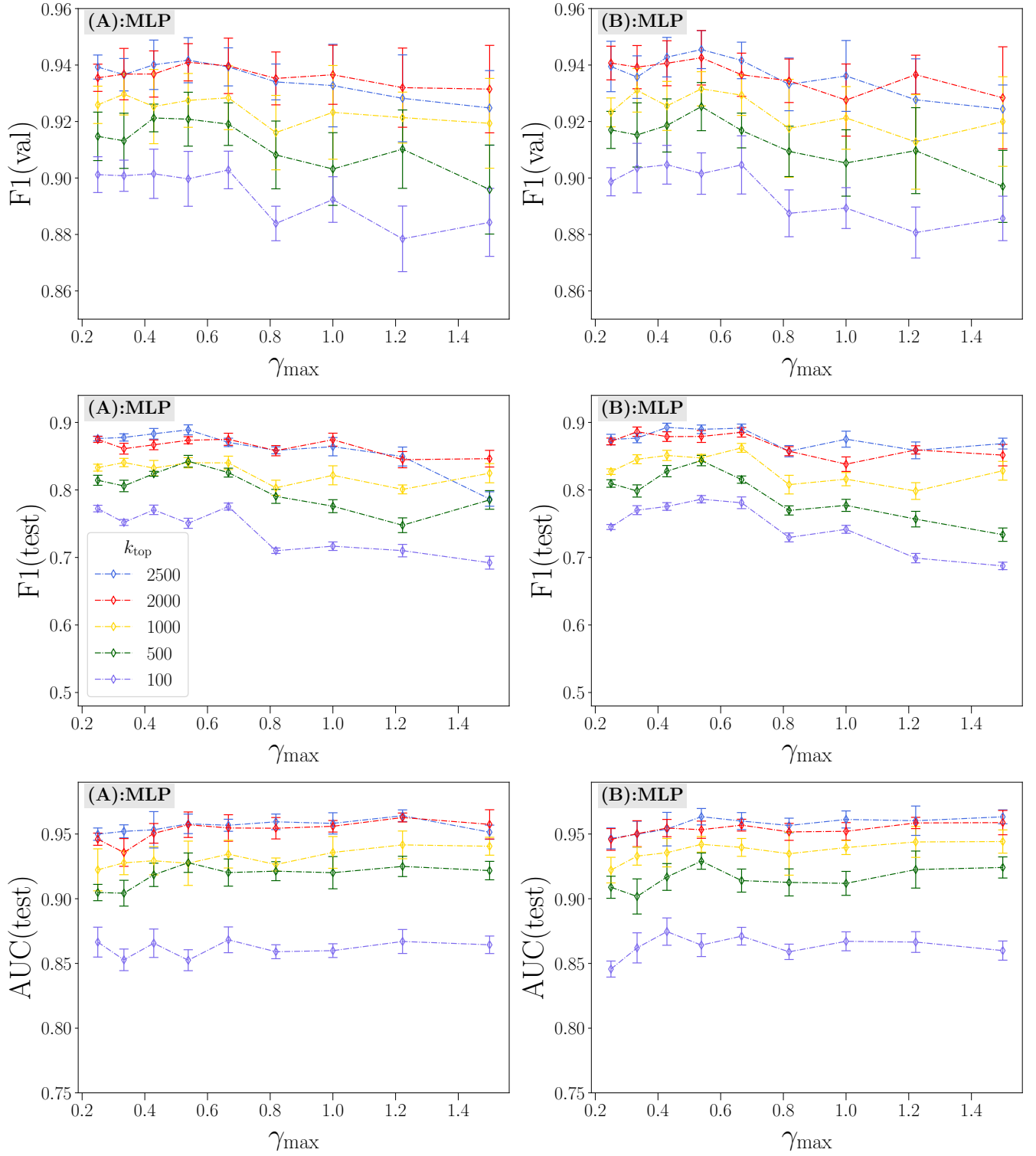


Figure 3. Top to bottom: Aggregated F1(val), F1(test), and AUC(test) for inter-operation (**A**, left column) and inter-operation (**B**, right column) classification with varying γ_{\max} and k_{top} . Errors are calculated from individual subtasks (**A1**, **A2**, **A3** and **B1**, **B2**, **B3**) using uncertainty propagation.

2.2 Coordination analysis of composite dataset

In order to understand intra- and inter-operation patterns of coordination, we report co-URL counts between all campaigns in Figure 4. The 2x2 block pattern of co-URL counts along the diagonal of 4a and 4b suggests that each campaign of a particular origin is actually a continuation of the same underlying operation. Observing how these co-URLs are distributed as a function of interarrival time, we see that the earlier identified training campaigns in 4c have similar distributions of co-URLs as the later identified test campaigns in 4c in some cases. In particular, the campaigns of Chinese and Iranian origin appear to adopt near-simultaneous link sharing later than the Russian campaigns. This can be quantified by calculating the distance between CDFs for each campaign (4e). From 4f, we see that the accounts in the Chn.(19) and Iran(19) campaigns appear to use little to no coordination at short timescales compared to the baseline, but the Chn.(20) and Iran(21) campaigns begin to display levels of coordination comparable to the Rus.(18) campaign. The Rus.(20) campaign displays greater levels of coordination than any campaign in our dataset, particularly at short timescales.

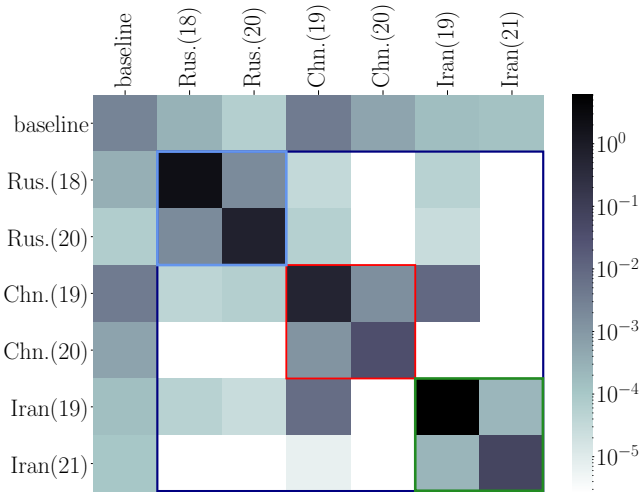
2.3 Feature Importance

For each model and subtask, we report the best performing graph encoding in each case (G.E. in Table 2). However, it is not clear from these results what the relative importance of each graph-based feature is on model predictions, or the relative importance of content-based to graph-based features. To quantify the relative importance of each feature set, we calculate the mean absolute integrated gradients (IG) for each feature over validation, test, and baseline sets for each subtask (Table 4 in the Appendix). In Table 3 we report the aggregated (arithmetic mean) IG values of each feature over all subtasks. We again use MLP as a representative model since it consistently performs well on all subtasks.

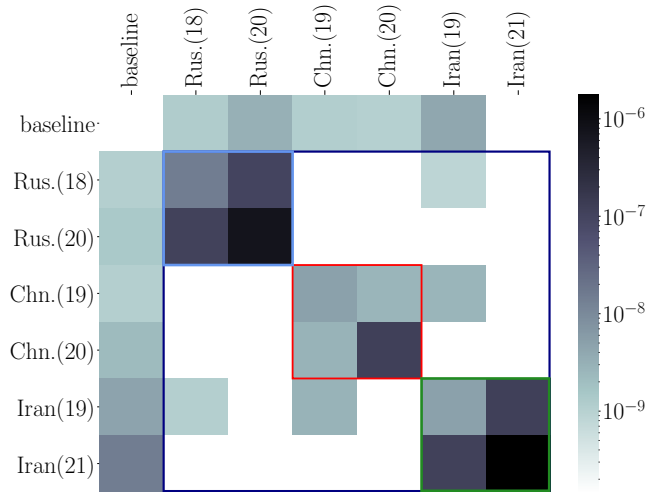
Overall, the net attribution of all graph-based features (**node2vec**, **LE**, **RWPE**, **NF**) appears to be substantially larger than that of all content-based features (**domains**), greater by roughly an order of magnitude. Notably, several quantities widely used in network analysis such as Laplacian Eigenmaps (**LE**), clustering coefficient, and betweenness centrality had a marginal impact on predictions, indicating that they provided little useful information for predictions and, since dropout was employed, that this information was not even redundant with other features. Meanwhile, graph embedding techniques such as **node2vec** and **RWPE** enjoy a relatively high utility, having a substantial impact on predictions. This result is not necessarily surprising since **node2vec** and **RWPE** essentially act as deep encoders, which can be decoded with high fidelity by deep neural networks (i.e. MLP and GNs, but not by LR and RF). What *is* surprising, on the other hand, is that several simple network quantities—degree, pagerank, and HITS—were as important to predictions as any other single feature. This implies that these quantities encode some information which is complementary to graph embedding techniques, and do so with only a single scalar value.

(A): Combined, intra-operation				(B): Combined, inter-operation			
feature	IG(val.)	IG(test)	IG(base.)	feature	IG(val.)	IG(test)	IG(base.)
domains	9.32×10^{-2}	1.06×10^{-1}	4.52×10^{-1}	domains	7.84×10^{-2}	9.31×10^{-2}	4.50×10^{-1}
node2vec	2.11×10^{-1}	3.42×10^{-1}	1.87×10^{-1}	node2vec	1.94×10^{-1}	3.38×10^{-1}	1.93×10^{-1}
LE	9.53×10^{-5}	5.32×10^{-4}	3.92×10^{-5}	LE	9.98×10^{-5}	5.18×10^{-4}	4.65×10^{-5}
RWPE	1.18×10^{-1}	2.83×10^{-1}	3.13×10^{-1}	RWPE	1.15×10^{-1}	2.87×10^{-1}	3.27×10^{-1}
NF	7.00×10^{-1}	8.68×10^{-1}	7.90×10^{-1}	NF	6.38×10^{-1}	8.36×10^{-1}	7.84×10^{-1}
degree	3.62×10^{-1}	3.02×10^{-1}	2.60×10^{-1}	degree	3.31×10^{-1}	2.97×10^{-1}	2.65×10^{-1}
cluster. coef.	9.51×10^{-3}	1.56×10^{-3}	7.34×10^{-3}	cluster. coef.	4.92×10^{-3}	3.17×10^{-3}	7.22×10^{-3}
betweenness	1.39×10^{-3}	4.04×10^{-2}	7.83×10^{-2}	betweenness	3.65×10^{-3}	3.97×10^{-2}	8.08×10^{-2}
pagerank	1.75×10^{-1}	2.87×10^{-1}	3.60×10^{-1}	pagerank	1.58×10^{-1}	2.74×10^{-1}	3.60×10^{-1}
HITS	1.45×10^{-1}	2.20×10^{-1}	7.74×10^{-2}	HITS	1.35×10^{-1}	2.21×10^{-1}	7.10×10^{-2}

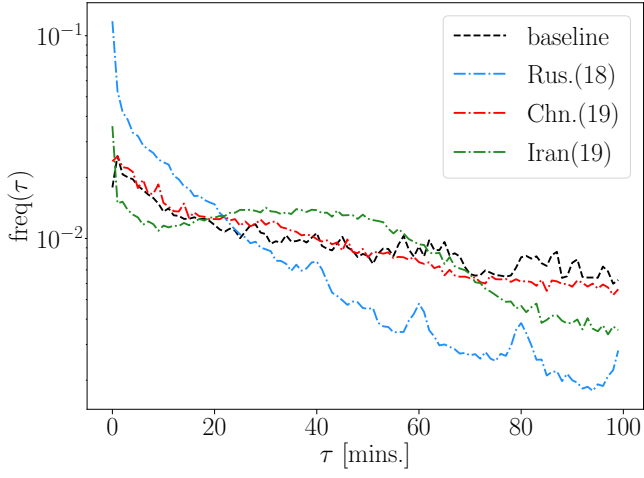
Table 3. Mean absolute integrated gradients (IG) of trained MLPs over features for validation, test, and baseline subsets. For all features, we report the sum of absolute values to avoid cancellation due to conflicting signs. Additionally, we report the IG of each of the five quantities comprising (**NF**). For IG values of individual subtasks and domains, see Tables 4 and 5 in the Appendix.



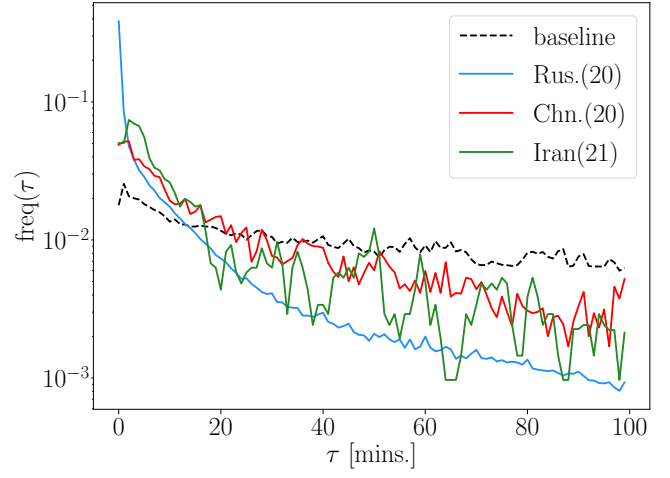
(a) Frequency of co-URLs between each subset. Counts are normalized by the size of the leading and lagging subsets.



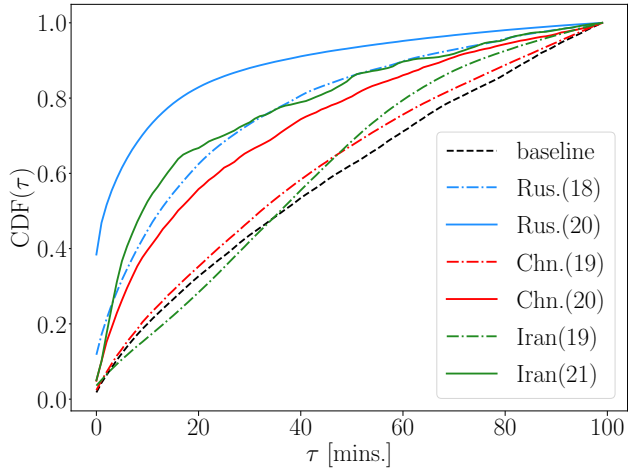
(b) Frequency near-simultaneous co-URLs ($\tau < 1$ min.) between subsets. Counts are normalized by the size of the leading and lagging subsets.



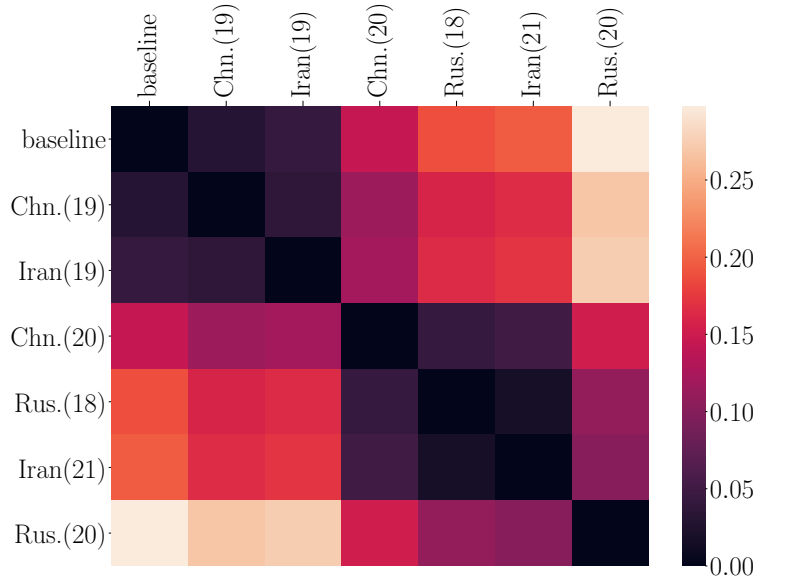
(c) Training set co-URL counts as a function of interarrival time τ . Each series corresponds to a diagonal element in Figure 4a and 4b above.



(d) Test set co-URL counts as a function of interarrival time τ . Each series corresponds to a diagonal element in Figures 4a and 4b above.



(e) Cumulative distribution function of co-URL counts for all campaigns.



(f) Mean absolute distance between CDFs. An increase in near-simultaneous link sharing was observed across operations even as automated detection improved.

Figure 4. Summary of co-URL statistics for the 6 IO subsets and baseline.

3 Discussion

Constraining influence operations is an ongoing challenge that will require continued advancement of detection capabilities in order to counter novel operations—particularly as they adopt powerful AI technologies. In particular, detection methods which go beyond established transductive methodologies and can identify novel campaigns in an inductive manner will be critical. Here we have examined the systematic application of generalized indicators and graph learning techniques, demonstrating a framework in Figure 5 which enhances detection coverage. Furthermore, this framework is broadly applicable to detecting manipulation on social media, and naturally complements detection using technical indicators identified in transductive methodologies.

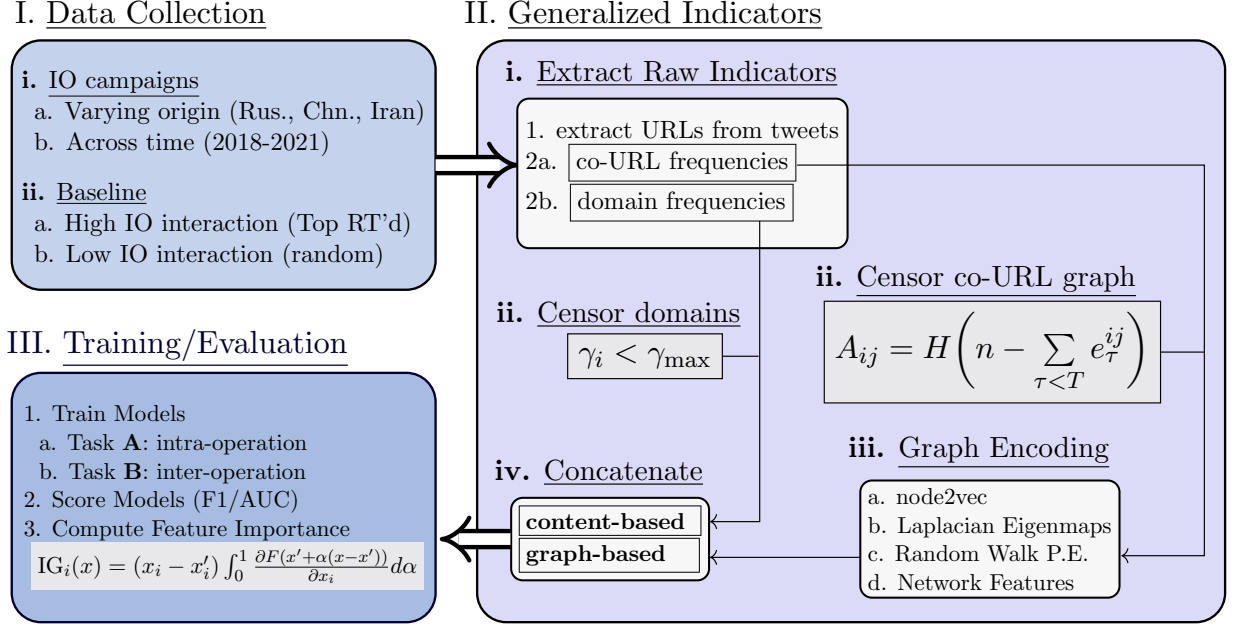


Figure 5. Illustration of the proposed inductive learning framework for the detection of information operations: **I.**) Collect IO data spanning various operations and time periods, as well as a baseline that interacts with the IO to varying degrees; **II.**) Extract and censor raw content-based and graph-based indicators and encode signatures of coordination via graph learning; **III.**) Evaluate model performance on tasks requiring generalization and determine the most important indicators using feature attribution. $H(\cdot)$ is the Heaviside step function.

Overall, the most effective approaches utilized: (1) a fairly large content-based feature set (approximately 2000-2500 domains) with fairly stringent removal threshold applied ($\gamma_{\max} \approx 0.5$); (2) a broad range of graph-encoding features, particularly **node2vec**, **RWPE**, degree, pagerank, and HITS; (3) a deep neural architecture. In other words, MLP and the three GNs outperformed LR and RF on every out-of-sample subtask. On the in-sample prediction tasks, as quantified by F1(val) of tasks **A1**, **A2**, and **A3**, RF actually outperforms all of the deep models. It appears that in this case RF was simply able to memorize patterns specific to the training set, as it fails to generalize to the test set. For task **A**, this failure corresponds to ~ 5 point decrement on F1(test) and AUC(test) relative to the deep models. On task **B**, for which predictions had to be made by generalizing across campaigns, an even larger decrement of 10-15 points is observed across all metrics.

Among deep models, MLP consistently achieved high performance across all subtasks, achieving the highest AUC(test) in all cases but one. However, on all out-of-sample F1 scores one or more GNs outperformed MLP in all cases. This indicates that while GNs perform well at the decision boundary for classification (the naïve boundary $\alpha=0.5$ in all cases), misclassifications were by a greater margin than for MLP. This is possibly an indication that while the increased expressive power of GNs was beneficial for classifications on average, this could lead to even further errors on accounts which were the most difficult to classify.

While we have outlined several specific approaches for selecting feature sets and models which can generalize

across campaigns, there are a number of improvements which would likely further this work. First, there are presumably other sets of generalized indicators which may be in aid in out-of-sample identification of IO accounts. The first is text data, which we did not investigate. On one hand, text embeddings which encode specific narratives or ideologies could presumably provide useful information which is not necessarily specific to a particular IO campaign. But on the other hand, the length of text shared and the prevalence of text varies greatly among accounts even with a single platform, and even more so from platform to platform. For content-based features overall, a unified approach for encoding the content and semantics of text, images, audio and video would be ideal, since focusing on a specific form of content could lead to blind spots. For example, the multi-modal encoders used by the multi-task agent Gato [34] or the GPT-4 system [31] could allow for training on text posts and making inferences on video posts, and so on.

Though the co-URL is a effective and robust tool for quantifying coordination, there are many other edge-wise features e_{ij} which quantify pair-wise relationships in a graph. In particular, several graph-based measures which quantify similarity could add useful information: node-similarity measures based on nearest neighbors such as common neighbors, Jaccard Index, Adamic Adar, and preferential attachment coefficients; as well as path based measures such as shortest path lengths, Katz measure, and hitting time. Other similarity measures can be derived from graph learning measures by applying various distance metrics such as L_p , cosine, and Sørensen–Dice distances to pairs of graph encodings. Fortunately, message passing graph networks provide a natural way to incorporate similarity measures (or any edge-wise features) into predictions, making this type of extension straight forward.

Although we attempted to present a range of graph networks—convolutional, shallow message-passing, and deep message-passing graph networks—there are myriad design dimensions of graph networks which we did not explore. Among these are more advanced sampling strategies, attention mechanisms, and various message passing architectures. However, the results in this study are adequate to suggest that both graph learning and graph networks will be an indispensable tool for detecting IO into the future.

Finally, we examined a “hard” measure of coordination, the co-URL, in this paper. There could in the future, however, be softer forms of coordination which evade detection. For example, different URLs could lead to semantically or literally identical content, which would not be measured as coordination by our current approach. To hedge against this possibility, one could encode the content of URLs as embeddings and define coordination as a function of the distance between embeddings. This would generalize the current co-URL approach in which we implicitly assign identical URLs distance 0 and distinct URLs distance ∞ . This is yet another indication of the utility of multi-modal content encoders in future influence detection efforts.

In summary, we have demonstrated an inductive approach to detecting IO which allow for continued utility into the future and generalization capacity across campaigns, enabling identification beyond technical indicators identified by transductive methodologies. We have illustrated how specific content- and graph-based features realize these objectives, as well as how one can systematically identify these features. Finally, we have identified several refinements of the current approach, enabling continued advancement in the automated detection of IO even as these campaigns continue to evolve.

4 Methods

4.1 Data Collection and Inclusion Criteria

For the purpose of evaluating intra- and inter-operation generalization of machine learning models, we selected IO of several origins (Russia, China, and Iran) for which there were significant campaign sub-networks identified at different times. To this end, six Russian, Chinese, and Iranian origin campaigns identified by Twitter between 2018 and 2021 were suitable. Another important aspect considered was the availability of baseline accounts which both interacted with the IO (to provide adequate coordination measures) and remained independent of IO (to reduce bias in frequency measures). To this end the baselines of [17, 19] were used (88.5% of baseline accounts), in addition to 1129 accounts (11.5% of baseline accounts) highly interacted with by IO, as measured by co-URLs. Additionally, the 1129 high-interaction accounts were sampled at various maximum follower thresholds ($n = 10^2, 10^3$, and 10^4) since accounts with many followers ($n > 10^4$) were disproportionately interacted with by IO accounts. This resulted in an aggregate baseline which was highly connected to the IO and yet provided broad coverage of various types and sizes of accounts.

For this study, we focus specifically on IO accounts which displayed reasonably organic patterns of sharing, which evaded detection for some amount of time, and which could have reasonably had some impact on public discourse. We therefore selected from the initial data set accounts which: (1) were active for at least 3 months; (2) had at least 300 Tweets; (3) had at least 200 URL shares; (4) shared at least 5 unique domains; (5) had at least 10 co-URLs with at least 2 neighbors.

4.2 Extracting raw indicators

To obtain features from the raw tweet data, we expand all shortened URLs contained in tweets using the URLExpander library [35]. Then, to obtain domain counts for each account, we use the tldextract library to extract the domain of each URL tweeted by an account. We then generate node-wise and edge-wise features from the raw URLs and extracted domains:

Edge features: As a measure of coordination between accounts, we compute the interarrival time between shares of the same URL (co-URLs) and bin the results into 1 minute intervals to obtain a vector of co-URL frequencies between all pairs of accounts. Denoting the interarrival time as τ , the co-URL count between the i th and j th account in the interarrival window $\tau - 1 < t \leq \tau$ is then denoted e_{τ}^{ij} .

Node features: We use the raw counts of the most frequently shared top-level domains (e.g., cnn.com, youtube.com, nytimes.com) from each account in the composite dataset. To avoid having the models simply memorize domains which are specific to a particular IO, we censor domains where more than γ_{\max} of occurrences of the domain originate from the IO training set relative to the baseline set. For example, riafan.ru, histantv.com, and tel-avivtimes.com are censored by this method for any $\gamma_{\max} < 10^4$ since each of these domains originate at least 10^4 more frequently from IO accounts than from the baseline. See Appendix E for extended examples of censored domains.

Graph Encoding: From a censored co-URL graph we compute three graph embeddings—node2vec (dim= 128), Laplacian Eigenmaps (dim= 50), Random Walk Positional Encodings (dim= 50), and several network statistics (degree, clustering coefficient, betweenness centrality, PageRank and HITS). We define the concatenation of all graph-based features the graph encoding.

4.3 Content-based generalized indicators

Following transductive methodologies, previous work has enabled the rapid detection of IO which attempt to propagate specific domains containing fake news, propaganda, and malware [7, 10, 27]. Accounts sharing these domains, particularly in a coordinated manner, are now routinely identified and removed by mainstream platforms. To identify influence efforts beyond these more flagrant indicators, we investigate domains which are commonly shared and yet may be useful indicators of IO activity. In order to quantify the extent to which a particular domain is either common to some baseline users or specific to an IO, we define the relative frequency for the i th domain in the IO training set ($y = 1$) relative to a baseline set ($y = 0$) as

$$\gamma_i = \frac{\text{tf}(i, y = 1)}{\text{tf}(i, y = 0)} \quad (1)$$

where the domain term frequencies for the i th domain are

$$\begin{aligned} \text{tf}(i, y = 1) &= \frac{f_i^{(y=1)}}{\sum_i f_i^{(y=1)}} \\ \text{tf}(i, y = 0) &= \frac{f_i^{(y=0)}}{\sum_i f_i^{(y=0)}} \end{aligned} \quad (2)$$

and $f_i^{(y=1,0)}$ are the raw counts of the i th domain in the IO and baseline training sets. We then censor any domains which exceed a threshold γ_{\max} such that we remove domains which are specific to the IO training set with variable stringency. Particular choices of γ_{\max} can censor domains which only appear in the baseline set ($\gamma_{\max} = 0$), appear in the IO set no more than parity ($\gamma_{\max} = 1$), or which appear only in the IO set ($\gamma_{\max} = \infty$). Additionally, we retain only a select number of the censored domains, k_{top} , the top- k domains when sorted in descending order by absolute frequency. We can then vary the stringency and minimum prevalence of our content-based feature set with γ_{\max} and k_{top} , respectively, in order to investigate the effect of content censorship on generalization. Moreover, at less stringent thresholds ($\gamma_{\max} > 1$), we can observe the effect of directly including technical indicators of previous campaigns used in transductive methodologies.

4.4 Graph-based generalized indicators

Coordination by IO on social platforms has taken many forms, including mass spamming, mass reporting, and coordinated content sharing. Among these tactics, coordinated content sharing has perhaps been the most widely observed, and is the chief tactic employed by many campaigns. In particular, many takedown efforts have used near-simultaneous co-URL sharing as the primary means of both identifying and substantiating coordinated inauthentic behaviour. In addition to the ubiquity of co-URLs across a variety of campaigns and platforms, they also have the appealing properties that they are agnostic to the specific content shared, are easily defined across platforms, and automatically imply a graph structure between accounts. Furthermore, each co-URL has an associated time between shares, the *interarrival time*, whose distribution can provide further insight into coordinated activity between accounts (see Figure 4 for examples).

While near-simultaneous co-URLs are a useful indicator for automated detection of IO activity, this behaviour is not guaranteed to persist, particularly for campaigns with high operational security (i.e., those which closely mimic authentic users). Therefore, generalized indicators of coordination should incorporate a broader time frame within which future campaigns are likely to operate. In particular, we utilize co-URLs with interarrival times from $\tau = 0$ to 100 minutes. This time frame includes near-simultaneous sharing (<1 min.), the majority of retweets (<20 min. [36]), and the median half-life of tweet views (~ 80 mins. [37]). We denote the number of co-URLs with interarrival times $\tau - 1 < t \leq \tau$ as e_τ^{ij} , and the composite co-URL vector as $e_{ij} = \{e_1^{ij}, \dots, e_{100}^{ij}\}$.

The graph structure implied by co-URLs, however, cannot be used directly by machine learning models to make node-wise inferences. Two approaches for utilizing graph structured data in machine learning applications are to: (i) learn unsupervised feature vectors for each node in the graph (*graph embedding*); and/or (ii) define graph operators which systematically aggregate data over the graph at each layer in a neural network. Both of these techniques can be referred to collectively as *graph learning* [38], and neural networks utilizing graph operators as *graph networks*.

Graph networks can utilize co-URL data in ways which may or may not directly make use of near-simultaneous link sharing behaviour, thereby offering varying degrees of generalization capacity. For example, one can define a graph which censors near-simultaneous link sharing as follows: assign $A_{ij} = 1$ if and only if two accounts share at least n URLs with interarrival times less than T , or in mathematical notation

$$A_{ij} = H\left(n - \sum_{\tau < T} e_\tau^{ij}\right) \quad (3)$$

where $H(\cdot)$ is the Heaviside step function. This definition equally counts the contribution of all co-URLs with interarrival times less than T , thereby censoring any near-simultaneous behavior while still allowing a rigorous threshold for coordination. One can then define graph operators, such as GCN [39], in terms of this censored graph. A standard way of directly using vector-valued edge features such as co-URLs, on the other hand, is within a message passing [40, 41] framework. Message passing defines graph operators directly as a function $\phi(e_{ij})$ of the edge-wise feature vectors (i.e., allowing predictions to be made directly using near-simultaneous co-URLs e_1^{ij}). In order to understand the generalization capacity of graph networks with varying degrees of graph censorship, we implement three graph networks as follows: GCN, which utilizes only the censored graph; MP-GCN(s), a message passing variant of the base GCN architecture with a shallow message passing function $\phi = L$, where L is a linear operator; and MP-GCN, which uses the more common deep message passing function $\phi = f$, where f is a neural network. Comparing the performance of these three architectures allows us to examine the effect of graph censorship, as well as compare different graph network architectures in identifying IO.

4.5 Graph Encoding

In order to understand the utility of different types of graph-based features (from network analysis to graph learning) as well as the utility of specific features, we incorporate several candidate quantities in a node-wise feature vector which we call the graph encoding. Due to the asymmetric nature of our dataset (co-shares of content *by* IO accounts are visible in the dataset, but co-shares *of* IO account content have been removed by Twitter) we treat all graph quantities in an undirected manner by setting $e_{ij} \leftarrow e_{ij} + e_{ji}$. All graph-based features are derived from an undirected graph computed from the co-URL vectors as in Equation 3 where we select thresholds of $n = 10$ and $T = 15$ to censor the graph. While more stringent n would produce a more robust graph, we find that further reducing the number of edges rapidly disjoints the graph, making graph learning techniques infeasible. The temporal threshold $T = 15$ minutes represents a window in which IO could coordinate effectively and yet avoid detection, while also censoring near-simultaneous link sharing.

Graph representation learning, including graph embedding algorithms such as node2vec [42], originated as an effort to automate the feature engineering process for graph prediction tasks such as node classification and link

prediction. From a modern perspective, graph embedding techniques are unsupervised methods which allow one to systematically assign relational, functional, and structural information to each node in a graph. This information can greatly improve the performance of deep learning models, with or without graph operators, on graph prediction tasks. We choose three graph embedding algorithms for our purpose here: (1) node2vec, which encodes neighborhood information of nodes into dense embeddings; (2) Laplacian Eigenmaps, a non-linear spectral embedding technique which provides a local coordinate system on graphs and effectively encodes clustering within the graph; (3) Random Walk Positional Encoding, which is based on the graph diffusion operator and uniquely assigns node embeddings based on the k -hop topological neighborhood of each node. Each of these approaches, in principle, encode different aspects of graph topology and therefore can provide predictive utility independent of one another. In each case, the dimensions of the embeddings are chosen such that further increases yield no benefit to performance across models.

While graph embeddings are a sensible method of encoding topological information for predictive tasks, they do not necessarily preclude the utility of conceptually similar network analysis quantities. To this end we include several quantities which encode relational, functional, and structural information of graphs in our graph encoding: (1) degree, which for undirected graphs is simply the number of directly adjacent neighbors of each node; (2) clustering-coefficient, which quantifies the local clustering of each node as the amount of closure between the neighbors of each node; (3) betweenness centrality, a centrality measure quantifying the extent to which a node facilitates connection within the graph via shortest paths; (4) pagerank, a centrality measure which ranks nodes according to their relative importance within a network; (5) HITS, which also ranks nodes according to relative importance but assigns two scores quantifying the extent to which a node connects the graph (hub score) and is of relative importance within the graph (authority score). For undirected graphs, the hub and authority scores of HITS are identical.

4.6 Graph Networks

Given the node-wise and edge-wise data in our feature set, there are several GN architectures which are possible choices for the predictive task at hand. We sample several architectures of increasing expressive power such that we can compare the utility of different GN design choices and degrees of graph censorship. In particular, we perform ablation on message-passing rules for encoding the co-URL vectors e_r^{ij} in order to compare various uses of this feature set.

In general, a graph network can be written as the series of operations

$$h_i^{(l+1)} = W^{(l)}h_i^{(l)} + b^{(l)} \quad (\text{affine transformation}) \quad (4)$$

$$h_i^{(l+1)} = \text{AGG}_{j \in \mathcal{N}(i)} \left(h_j^{(l+1)} \right) \quad (\text{feature aggregation}) \quad (5)$$

$$h_i^{(l+1)} = \sigma \left(h_i^{(l+1)} \right) \quad (\text{non-linearity}) \quad (6)$$

where the set $\mathcal{N}(i)$ indicates the neighborhood of the i th node where $A_{ij} = 1$. The simplest graph network that we employ is a spectral GN, the popular Graph Convolutional Network (GCN), with layers defined by the feature aggregation function [39]

$$\text{AGG} = \sum_{j \in \mathcal{N}(i)} \frac{1}{\sqrt{d_i d_j}} h_j^{(l+1)} \quad (\text{GCN}) \quad (7)$$

where d_i is the degree of the i th node.

There are a number of ways in which message passing rules can be defined, but for graph networks one typically defines the message passing rule as

$$m_{ij}^{(l+1)} = \phi \left(h_i^{(l)}, h_j^{(l)}, e_{ij} \right) \quad (8)$$

where the message passing function $\phi(\cdot)$ can take as input both nodewise features $h_i^{(l)}$ and edgewise features e_{ij} . We then incorporate these messages into the aggregation step as

$$h_i^{(l+1)} = \text{AGG}_{j \in \mathcal{N}(i)} \left(h_j^{(l+1)}, m_{ij}^{(l+1)} \right) \quad (9)$$

We employ two message passing rules to encode the co-URL vector, the first of which is a shallow message passing rule which defines our MP-GCN(s):

$$m_{ij}^{(l+1)} = \sigma \left(\sum_{\tau} w_{\tau}^{(l)} e_{\tau}^{ij} \right). \quad (10)$$

The second rule utilizes a neural message passing function, implemented as an L layer perceptron which defines our MP-GCN:

$$\begin{aligned} a_{ij}^{(k+1)} &= \sigma \left(W^{(k,l)} a_{ij}^{(k)} + b^{(k,l)} \right); \\ m_{ij}^{(l+1)} &= \sigma \left(W^{(L)} a_{ij}^{(L)} + b^{(L)} \right); \end{aligned} \quad (11)$$

where $W^{(l)}$ and $b^{(l)}$ are the weights and biases of the l th layer and $a_{ij}^{(0)} = e_{\tau}^{ij}$. To compare with the base GCN implementation, we insert each message passing rule into the base GCN aggregation function as

$$\text{AGG} = \sum_{j \in \mathcal{N}(i)} \frac{m_{ij} h_j^{(l+1)}}{\sqrt{d_i d_j}}. \quad (\text{MP-GCN(s)/MP-GCN}) \quad (12)$$

Thus we have performed ablation on the message passing rule over the three GCN architectures.

4.7 Model Training

In the LR and RF implementations we tune all hyperparameters to achieve the best model performance via gridsearch. In the MLP and the three GCN variants we use the same hyperparameters: two hidden layers of 64 units, and a dropout probability $p = 0.5$ applied to all units in the hidden layers. In all message passing layers we apply a dropout probability of $p = 0.2$. For all MLP and GCN training we use a binary cross entropy loss and the Adam optimizer with a learning rate of 10^{-4} .

4.8 Integrated Gradients

Integrated gradients [33] is an axiomatic attribution method for deep neural networks. Mathematically, the IG of a function $F(x)$ with respect to the i th component of an input x and a baseline x' is

$$\text{IntegratedGradient}_i(x) = (x_i - x'_i) \int_0^1 \frac{\partial F(x' + \alpha(x - x'))}{\partial x_i} d\alpha \quad (13)$$

where α parameterizes a straight line path from x' to x . This method provides a more robust attribution of predictions to specific features than directly evaluating the product of the gradient and feature value

$$\text{Attr}_i(x) = x_i \frac{\partial F}{\partial x_i} \quad (14)$$

which has historically been a popular attribution method. When using IG, one selects a baseline where the model prediction is neutral. Calculating the IGs of each feature for an MLP, there is not an obvious baseline which yields neutral predictions, i.e., where $F(x') = 0.5$. For example, simply choosing the mean or minimum value of each feature over various subsets of the data produces predictions close to 0 or 1. We therefore construct an empirical baseline comprising the subset of all nodes such that $0.4 \leq F(x_j) \leq 0.6$, or within ± 0.1 of a neutral prediction. Setting $x' = \langle x_j \rangle$ then yields $F(x') = 0.534 \pm 0.018$ over all six subtasks, which is approximately neutral while ensuring that no particular feature in the baseline takes on an extreme value (which might be the case if we simply chose j to be the single most neutral prediction).

4.9 Error propagation of aggregated metrics

In Figure 3, several performance metrics are aggregated over subtasks by computing their harmonic mean. For each subtask and choice of parameters (γ_{\max} and k_{top}), there is an associated uncertainty for each metric due to their dependence on a random samples of train/validate/test splits in the data. In order to compare aggregated results for different parameter values, we propagate the uncertainties associated with each metric as follows. In general, the harmonic mean can be written

$$\hat{x} = \frac{n}{\sum_{i=1}^n x_i^{-1}} \quad (15)$$

and the propagated uncertainty (neglecting correlations between x_i)

$$\sigma_{\tilde{x}}^2 = \sum_{i=1}^n \left(\frac{\partial \tilde{x}}{\partial x_i} \right)^2 \sigma_{x_i}^2. \quad (16)$$

The partial derivatives of \tilde{x} with respect to each x_i are

$$\frac{\partial \tilde{x}}{\partial x_i} = \frac{\tilde{x}^2}{n} \frac{1}{x_i^2} \quad (17)$$

and the propagated uncertainty is then

$$\sigma_{\tilde{x}}^2 = \left(\frac{\tilde{x}^2}{n} \right)^2 \sum_{i=1}^n \left(\frac{\sigma_{x_i}}{x_i^2} \right)^2. \quad (18)$$

Using this result we can better understand different choices of γ_{\max} and k_{top} shown in Figure 3.

Code and data availability

Upon acceptance, code and data will be shared on an individual basis.

Acknowledgements

This material is based upon work supported by the Air Force Office of Scientific Research under award number FA9550-20-1-0382.

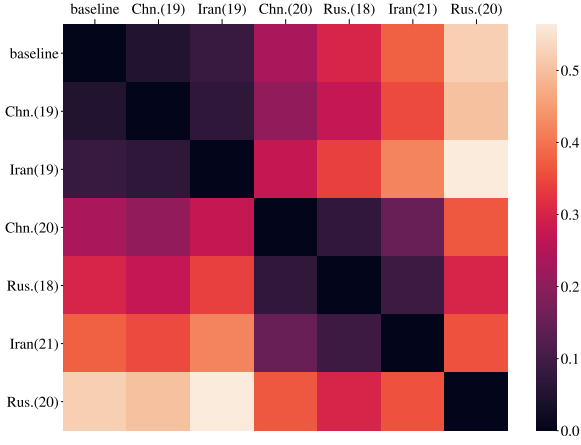
References

1. Broniatowski, D. A. *et al.* Weaponized health communication: Twitter bots and russian trolls amplify the vaccine debate. *Am. J. Public Heal.* **108** (2018).
2. Zannettou, S. *et al.* Who let the trolls out? towards understanding state-sponsored trolls. In *Proceedings of the 10th ACM Web Science*, 353–362 (2019).
3. Zhou, Y., Dredze, M., Broniatowski, D. A. & Adler, W. D. Elites and foreign actors among the alt-right: The gab social media platform. *First Monday* (2019).
4. Linvill, D. L. & Warren, P. L. Troll factories: Manufacturing specialized disinformation on twitter. *Polit. Commun.* **37**, 447–467 (2020).
5. Rossetti, M. & Zaman, T. Bots, disinformation, and the first impeachment of US president Donald Trump. *PloS one* **18**, e0283971 (2023).
6. Nimmo *et al.* Taking down coordinated inauthentic behavior from Russia and China. *Meta Newsroom* (2022).
7. Nimmo *et al.* Quarterly adversarial threat report (Q2). *Meta Newsroom* (2022).
8. Meta. Quarterly adversarial threat report (Q3). *Meta Newsroom* (2022).
9. Nimmo *et al.* Quarterly adversarial threat report (Q4). *Meta Newsroom* (2023).
10. Meta. Quarterly adversarial threat report (Q1). *Meta Newsroom* (2022).
11. Twitter Safety. Disclosing networks of state-linked information operations we’ve removed. *Twitter Blog* (2020).
12. Twitter Safety. Disclosing networks of state-linked information operations. *Twitter Blog* (2021).
13. Etudo, U., Yoon, V. Y. & Yaraghi, N. From facebook to the streets: Russian troll ads and black lives matter protests. In *Proceedings of the 52nd Hawaii International Conference on System Sciences* (2019).
14. Hurtado, S., Ray, P. & Marculescu, R. Bot detection in reddit political discussion. In *Proceedings of the Fourth International Workshop on Social Sensing*, 30–35 (2019).
15. Zannettou, S. *et al.* Characterizing the use of images in state-sponsored information warfare operations by russian trolls on twitter. In *Proceedings of the International AAAI Conference on Web and Social Media* (2020).
16. Smith, S. T. *et al.* Automatic detection of influential actors in disinformation networks. *Proc. Natl. Acad. Sci.* **118** (2021).

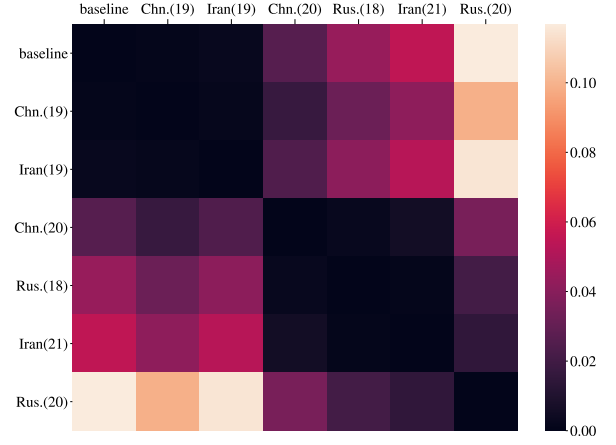
17. Alizadeh, M., Shapiro, J. N., Buntain, C. & Tucker, J. A. Content-based features predict social media influence operations. *Sci. Adv.* **6** (2020).
18. Monti, F., Frasca, F., Eynard, D., Mannion, D. & Bronstein, M. M. Fake news detection on social media using geometric deep learning. *CoRR* **abs/1902.06673** (2019).
19. Vargas, L., Emami, P. & Traynor, P. On the detection of disinformation campaign activity with network analysis. *Proc. ACM SIGSAC Conf. on Cloud Comput. Secur.* (2020).
20. Nimmo, B. & Hutchins, E. Phase-based tactical analysis of online operations. *Carnegie Endowment for International Peace* (2023).
21. Pols, P. The unified kill chain. *Fox-IT* (2017).
22. Sedova, K. *et al.* AI and the future of disinformation campaigns, part 1: The richdata framework. *Georgetown Center for Security and Emerging Technology* (2021).
23. Graphika & The Stanford Internet Observatory. Bad reputation. *Graphika Reports* (2022).
24. Giglietto, F., Righetti, N., Rossi, L. & Marino, G. It takes a village to manipulate the media: coordinated link sharing behavior during 2018 and 2019 italian elections. *Information, Commun. & Soc.* **23**, 867–891 (2020).
25. Facebook. Threat report: The state of influence operations 2017-2020. *Meta Newsroom* (2021).
26. Das Sarma, A. *et al.* Ranking mechanisms in twitter-like forums. *Proc. Third ACM WSDM* (2010).
27. Graphika. Deepfake it till you make it. *Graphika Reports* (2023).
28. Nimmo *et al.* Secondary infection. *Graphika Reports* (2020).
29. Karras, T. *et al.* Analyzing and improving the image quality of stylegan. *CoRR* **abs/1912.04958** (2019).
30. Perov, I. *et al.* Deepfacelab: A simple, flexible and extensible face swapping framework. *CoRR* **abs/2005.05535** (2020).
31. OpenAI. Gpt-4 technical report. *CoRR* **abs/2303.08774** (2023).
32. Ramesh, A. *et al.* Zero-shot text-to-image generation. *CoRR* **abs/2102.12092** (2021).
33. Sundararajan, M., Taly, A. & Yan, Q. Axiomatic attribution for deep networks. *CoRR* **abs/1703.01365** (2017).
34. Reed, S. *et al.* A generalist agent. *Transactions on Mach. Learn. Res.* (2022).
35. Yin, L. Smappnyu/urlxpander: Initial release (2018).
36. Yin, H., Yang, S., Song, X., Liu, W. & Li, J. Deep fusion of multimodal features for social media retweet time prediction. *World Wide Web* **24**, 1027–1044 (2021).
37. Pfeffer, J., Matter, D. & Sargsyan, A. The half-life of a tweet. *CoRR* **abs/2302.09654** (2023).
38. Chami, I., Abu-El-Haija, S., Perozzi, B., Ré, C. & Murphy, K. Machine learning on graphs: A model and comprehensive taxonomy. *J. Mach. Learn. Res.* **23**, 1–64 (2022).
39. Kipf, T. N. & Welling, M. Semi-supervised classification with graph convolutional networks. *CoRR* **abs/1609.02907** (2016).
40. Gilmer, J., Schoenholz, S. S., Riley, P. F., Vinyals, O. & Dahl, G. E. Neural message passing for quantum chemistry. *Proc. Mach. Learn. Res.* **70**, 1263–1272 (2017).
41. Dwivedi, V. P., Luu, A. T., Laurent, T., Bengio, Y. & Bresson, X. Graph neural networks with learnable structural and positional representations. *CoRR* **abs/2110.07875** (2021).
42. Grover, A. & Leskovec, J. node2vec: Scalable feature learning for networks. *CoRR* **abs/1607.00653** (2016).

A Additional CDF distance metrics

Here we show additional metrics for the CDF distances shown in Figure 4. We see that these demonstrate a similar pattern as the mean absolute distance shown in 4f, though Mean Squared Distance demonstrates stronger clustering.



(a) Kolmogorov-Smirnov distance between each CDF in Figure 4e.



(b) Mean Squared Distance between each CDF in Figure 4e.

B Subtask F1(val/test) and AUC(test) for varying γ_{\max} and k_{top}

We show here individual results for F1(val), F1(test), and AUC(test). In the top 2 panels of each figure, we show the aggregated results of Figure 3, and in the lower 6 panels we show the subtask results from which these are computed (as the harmonic mean).

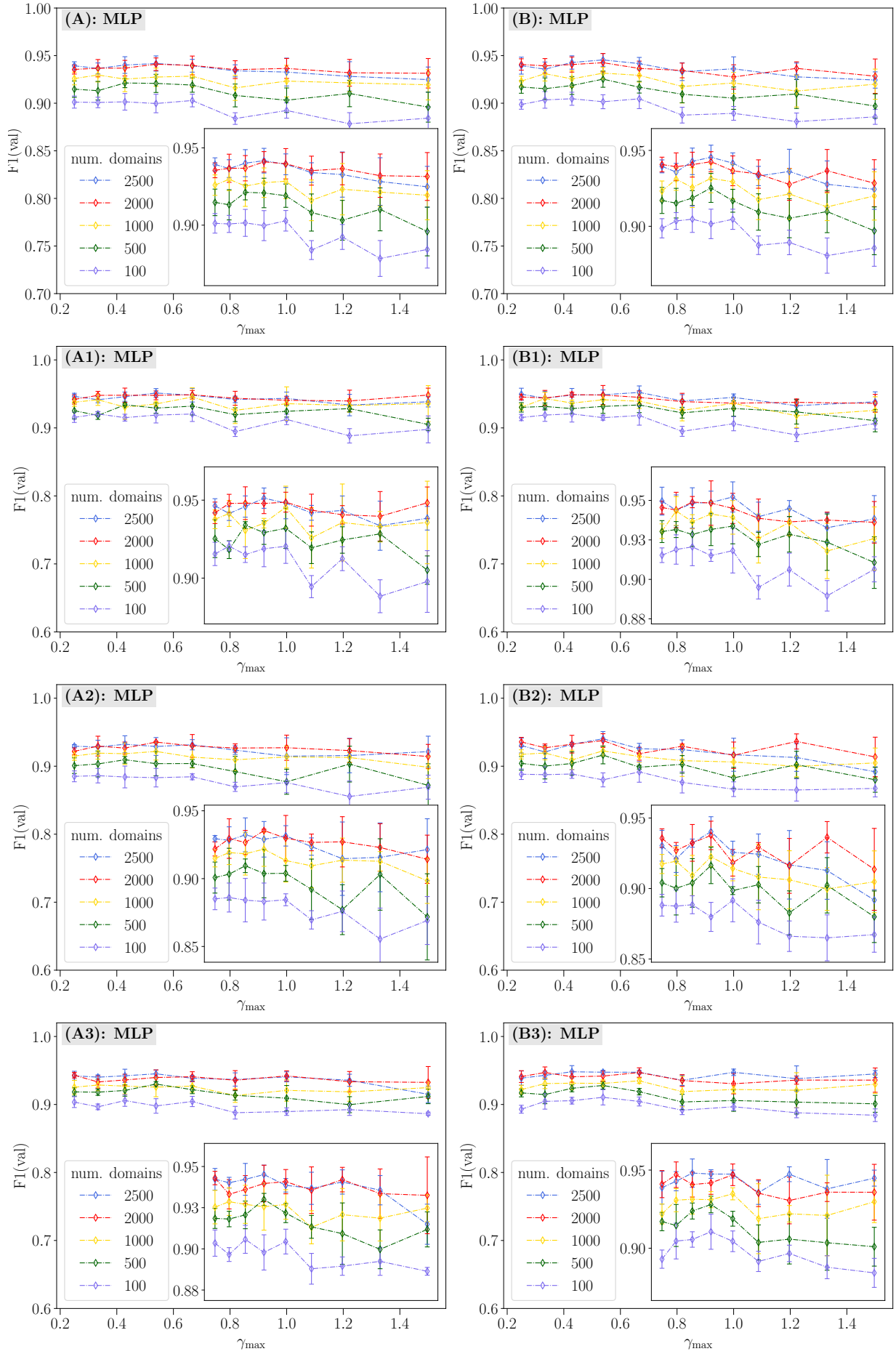


Figure 7. F1(val) for aggregated tasks (top two panels) and subtasks (bottom six panels). **Inset:** Series replotted with a rescaled y -axis.

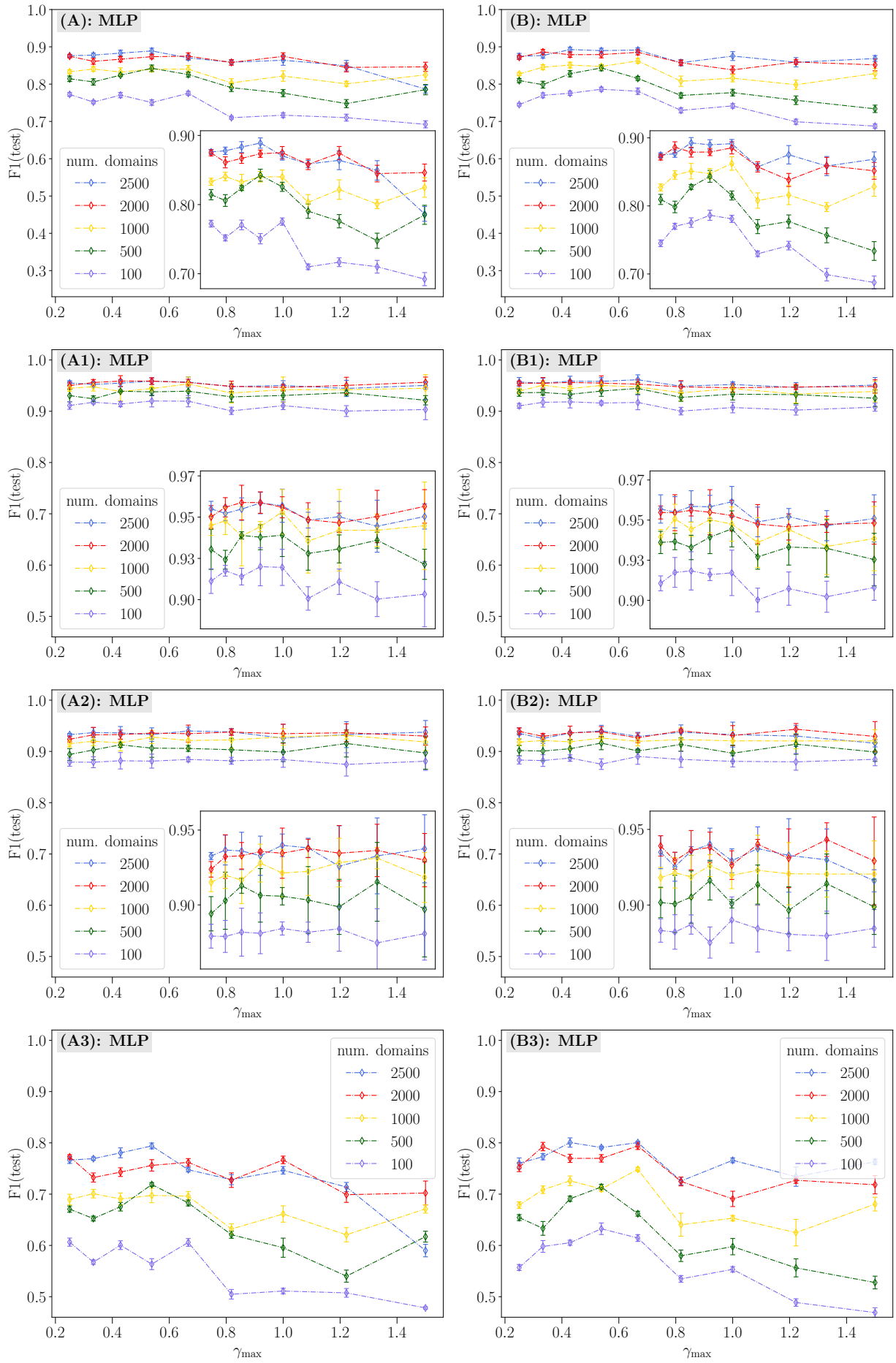


Figure 8. F1(test) for aggregated tasks (top two panels) and subtasks (bottom six panels). **Inset:** Series replotted with a rescaled y -axis.

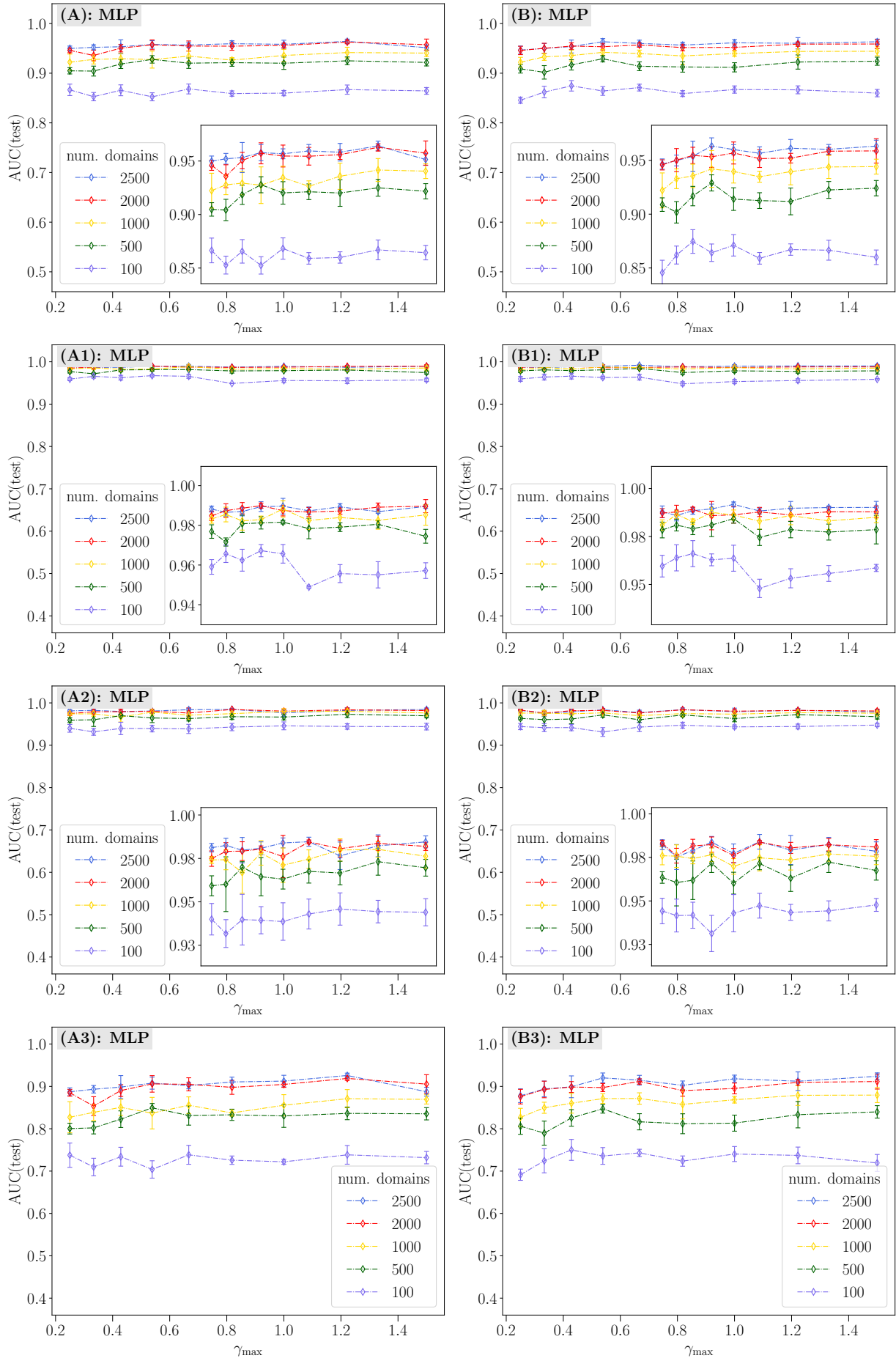


Figure 9. AUC(test) for aggregated tasks (top two panels) and subtasks (bottom six panels). **Inset:** Series replotted with a rescaled y -axis.

C Subtask level integrated gradients

In Table 3, we show the mean IG values over subtasks. Here we show explicit results for each of these subtasks. The subtask level results are largely consistent with the aggregated results, although attributions for individual features can vary by up to $\pm 20\%$ across subtasks.

(A1): Rus(18) \rightarrow Rus(18) / Rus(20)

(B1): Chn(19) + Iran(19) \rightarrow Rus(18) / Rus(20)

feature	IG(val.)	IG(test)	IG(base.)	feature	IG(val.)	IG(test)	IG(base.)
domains	9.44×10^{-2}	5.21×10^{-2}	4.61×10^{-1}	domains	9.79×10^{-2}	4.84×10^{-2}	4.78×10^{-1}
node2vec	1.54×10^{-1}	3.40×10^{-1}	1.98×10^{-1}	node2vec	1.51×10^{-1}	3.39×10^{-1}	2.09×10^{-1}
LE	8.87×10^{-5}	1.26×10^{-4}	4.16×10^{-5}	LE	1.04×10^{-4}	1.31×10^{-4}	4.93×10^{-5}
RWPE	7.44×10^{-2}	1.77×10^{-1}	3.23×10^{-1}	RWPE	7.26×10^{-2}	1.74×10^{-1}	3.44×10^{-1}
NF	6.43×10^{-1}	7.09×10^{-1}	8.11×10^{-1}	NF	5.85×10^{-1}	6.40×10^{-1}	8.18×10^{-1}
degree	3.55×10^{-1}	3.44×10^{-1}	2.66×10^{-1}	degree	3.54×10^{-1}	3.45×10^{-1}	2.81×10^{-1}
cluster. coef.	1.70×10^{-2}	2.56×10^{-2}	3.34×10^{-2}	cluster. coef.	4.64×10^{-3}	3.48×10^{-3}	9.27×10^{-3}
betweenness	1.58×10^{-2}	2.97×10^{-3}	7.28×10^{-2}	betweenness	9.28×10^{-3}	5.13×10^{-3}	8.90×10^{-2}
pagerank	1.32×10^{-1}	1.78×10^{-1}	3.44×10^{-1}	pagerank	1.19×10^{-1}	1.66×10^{-1}	3.70×10^{-1}
HITS	1.23×10^{-1}	1.58×10^{-1}	9.43×10^{-2}	HITS	9.81×10^{-2}	1.21×10^{-1}	6.91×10^{-2}

(A2): Chn(19) \rightarrow Chn(19) / Chn(20)

(B2): Rus(18) + Iran(19) \rightarrow Chn(19) / Chn(20)

feature	IG(val.)	IG(test)	IG(base.)	feature	IG(val.)	IG(test)	IG(base.)
domains	8.67×10^{-2}	1.23×10^{-2}	4.60×10^{-1}	domains	5.05×10^{-2}	1.38×10^{-2}	4.21×10^{-1}
node2vec	2.33×10^{-1}	2.76×10^{-1}	1.91×10^{-1}	node2vec	2.06×10^{-1}	3.13×10^{-1}	1.73×10^{-1}
LE	8.81×10^{-5}	2.71×10^{-4}	3.62×10^{-5}	LE	9.03×10^{-5}	3.42×10^{-4}	4.14×10^{-5}
RWPE	1.37×10^{-1}	2.97×10^{-1}	3.17×10^{-1}	RWPE	1.18×10^{-1}	3.05×10^{-1}	3.03×10^{-1}
NF	7.04×10^{-1}	7.74×10^{-1}	8.03×10^{-1}	NF	6.11×10^{-1}	8.58×10^{-1}	7.51×10^{-1}
degree	3.53×10^{-1}	2.45×10^{-1}	2.62×10^{-1}	degree	3.05×10^{-1}	2.78×10^{-1}	2.54×10^{-1}
cluster. coef.	6.56×10^{-3}	1.86×10^{-2}	6.04×10^{-3}	cluster. coef.	5.05×10^{-3}	1.36×10^{-2}	7.76×10^{-3}
betweenness	1.68×10^{-3}	3.41×10^{-2}	7.96×10^{-2}	betweenness	9.21×10^{-3}	4.90×10^{-2}	7.45×10^{-2}
pagerank	1.86×10^{-1}	2.73×10^{-1}	3.79×10^{-1}	pagerank	1.65×10^{-1}	3.09×10^{-1}	3.53×10^{-1}
HITS	1.57×10^{-1}	2.04×10^{-1}	7.74×10^{-2}	HITS	1.27×10^{-1}	2.09×10^{-1}	6.25×10^{-2}

(A3): Iran(19) \rightarrow Iran(19) / Iran(21)

(B3): Chn(19) + Rus(18) \rightarrow Iran(19) / Iran(21)

feature	IG(val.)	IG(test)	IG(base.)	feature	IG(val.)	IG(test)	IG(base.)
domains	9.86×10^{-2}	2.55×10^{-1}	4.34×10^{-1}	domains	8.67×10^{-2}	2.17×10^{-1}	4.51×10^{-1}
node2vec	2.47×10^{-1}	4.10×10^{-1}	1.71×10^{-1}	node2vec	2.25×10^{-1}	3.61×10^{-1}	1.97×10^{-1}
LE	1.09×10^{-4}	1.20×10^{-3}	3.98×10^{-5}	LE	1.05×10^{-4}	1.08×10^{-3}	4.88×10^{-5}
RWPE	1.44×10^{-1}	3.76×10^{-1}	3.00×10^{-1}	RWPE	1.55×10^{-1}	3.83×10^{-1}	3.33×10^{-1}
NF	7.54×10^{-1}	1.12×10^0	7.57×10^{-1}	NF	7.18×10^{-1}	1.01×10^0	7.83×10^{-1}
degree	3.79×10^{-1}	3.18×10^{-1}	2.52×10^{-1}	degree	3.33×10^{-1}	2.69×10^{-1}	2.60×10^{-1}
cluster. coef.	4.97×10^{-3}	2.32×10^{-3}	5.35×10^{-3}	cluster. coef.	5.06×10^{-3}	6.10×10^{-4}	4.63×10^{-3}
betweenness	9.96×10^{-3}	9.00×10^{-2}	8.25×10^{-2}	betweenness	7.53×10^{-3}	6.51×10^{-2}	7.88×10^{-2}
pagerank	2.06×10^{-1}	4.09×10^{-1}	3.57×10^{-1}	pagerank	1.91×10^{-1}	3.47×10^{-1}	3.58×10^{-1}
HITS	1.55×10^{-1}	2.97×10^{-1}	6.06×10^{-2}	HITS	1.81×10^{-1}	3.32×10^{-1}	8.14×10^{-2}

Table 4. IG values of individual subtasks.

D Integrated gradients by domain

Here we show the most significant domain level integrated gradients. We leave these values signed since they are largely consistent across data splits and subtasks. The signs do not necessarily indicate with certainty whether a feature was used to make a positive ($y = 1$) or negative ($y = 0$) prediction, though one expects a reasonable correspondence.

(A1): Rus(18) \rightarrow Rus(18) / Rus(20)

domain	IG(val.)	domain	IG(test)	domain	IG(base.)
untappd.com	4.65×10^{-3}	inc.com	-8.51×10^{-3}	nytimes.com	-2.08×10^{-2}
senate.gov	3.80×10^{-3}	soundcloud.com	5.06×10^{-3}	abouthub.info	-1.30×10^{-2}
nbcnews.com	2.35×10^{-3}	yahoo.com	-2.82×10^{-3}	conta.cc	-1.08×10^{-2}
tumblr.com	-2.33×10^{-3}	nbcnews.com	1.81×10^{-3}	politico.com	-1.08×10^{-2}
pscp.tv	1.85×10^{-3}	senate.gov	1.60×10^{-3}	senate.gov	9.19×10^{-3}
washingtonexam[*].com	1.82×10^{-3}	espn.com	-1.58×10^{-3}	abcnews.com	-6.90×10^{-3}
foursquare.com	-1.77×10^{-3}	techcrunch.com	-1.52×10^{-3}	reddit.com	-6.53×10^{-3}
furnishhome.ru	-1.71×10^{-3}	change.org	1.47×10^{-3}	github.com	-6.22×10^{-3}
house.gov	-1.65×10^{-3}	ebay.com	-1.39×10^{-3}	mailchimp.com	-5.98×10^{-3}
wordpress.com	-1.55×10^{-3}	foursquare.com	-1.21×10^{-3}	wsj.com	-5.95×10^{-3}
washingtonpost.com	-1.53×10^{-3}	usatoday.com	-1.18×10^{-3}	wabcradio.com	-5.86×10^{-3}
yahoo.com	-1.53×10^{-3}	nationalreview.com	9.91×10^{-4}	instagram.com	-5.78×10^{-3}
flwrs.com	-1.34×10^{-3}	washingtonpost.com	-9.65×10^{-4}	hubs.ly	-5.59×10^{-3}
twittascope.com	1.32×10^{-3}	smotrim.ru	-9.56×10^{-4}	foxnews.com	-5.54×10^{-3}
rawstory.com	-1.28×10^{-3}	sba.gov	9.19×10^{-4}	msn.com	-5.39×10^{-3}

(A2): Chn(19) \rightarrow Chn(19) / Chn(20)

domain	IG(val.)	domain	IG(test)	domain	IG(base.)
cnn.com	-2.88×10^{-3}	justunfollow.com	5.48×10^{-3}	nytimes.com	-2.08×10^{-2}
washingtonpost.com	-2.49×10^{-3}	etsy.com	-7.58×10^{-4}	abouthub.info	-1.30×10^{-2}
cdt.org	2.16×10^{-3}	tumblr.com	-5.40×10^{-4}	conta.cc	-1.08×10^{-2}
wordpress.com	-1.63×10^{-3}	yahoo.com	-4.56×10^{-4}	politico.com	-1.08×10^{-2}
wsj.com	-1.59×10^{-3}	cnn.com	-4.53×10^{-4}	senate.gov	9.19×10^{-3}
medium.com	-1.11×10^{-3}	foursquare.com	-3.83×10^{-4}	abcnews.com	-6.90×10^{-3}
bloomberg.com	9.32×10^{-4}	house.gov	-3.57×10^{-4}	reddit.com	-6.53×10^{-3}
eventbrite.com	-8.78×10^{-4}	medium.com	-3.50×10^{-4}	github.com	-6.22×10^{-3}
theconversation.com	7.66×10^{-4}	apnews.com	2.57×10^{-4}	mailchimp.com	-5.98×10^{-3}
yahoo.com	-7.61×10^{-4}	conservativejunc[*].com	2.54×10^{-4}	wsj.com	-5.95×10^{-3}
ap.org	7.39×10^{-4}	twittascope.com	2.25×10^{-4}	wabcradio.com	-5.86×10^{-3}
inewssource.org	6.83×10^{-4}	sba.gov	2.12×10^{-4}	instagram.com	-5.78×10^{-3}
www.gov.uk	-6.53×10^{-4}	theconversation.com	-1.62×10^{-4}	hubs.ly	-5.59×10^{-3}
mktw.net	-6.42×10^{-4}	wired.com	-1.36×10^{-4}	foxnews.com	-5.54×10^{-3}
sen.gov	-6.28×10^{-4}	github.com	-1.29×10^{-4}	msn.com	-5.39×10^{-3}

(A3): Iran(19) \rightarrow Iran(19) / Iran(21)

domain	IG(val.)	domain	IG(test)	domain	IG(base.)
huffpost.com	-4.25×10^{-3}	untappd.com	2.41×10^{-2}	nytimes.com	-1.83×10^{-2}
foursquare.com	-3.89×10^{-3}	gofundme.com	1.87×10^{-2}	abouthub.info	-1.12×10^{-2}
medium.com	-3.68×10^{-3}	twittascope.com	-1.34×10^{-2}	politico.com	-1.00×10^{-2}
untappd.com	3.58×10^{-3}	bbc.co.uk	1.24×10^{-2}	conta.cc	-9.88×10^{-3}
cnn.com	-3.09×10^{-3}	wired.com	-9.16×10^{-3}	senate.gov	9.27×10^{-3}
senate.gov	2.82×10^{-3}	iheart.com	8.79×10^{-3}	abcnews.com	-6.67×10^{-3}
house.gov	-2.66×10^{-3}	npr.org	8.12×10^{-3}	reddit.com	-5.96×10^{-3}
etsy.com	-2.41×10^{-3}	senate.gov	7.63×10^{-3}	wsj.com	-5.94×10^{-3}
apple.news	-2.34×10^{-3}	washingtonexaminer.com	6.55×10^{-3}	github.com	-5.58×10^{-3}
economist.com	2.19×10^{-3}	house.gov	-6.23×10^{-3}	mailchimp.com	-5.53×10^{-3}
abouthub.info	-2.14×10^{-3}	justunfollow.com	6.04×10^{-3}	wabcradio.com	-5.32×10^{-3}
yahoo.com	-2.13×10^{-3}	wordpress.com	-5.87×10^{-3}	hubs.ly	-5.23×10^{-3}
amazon.com	-2.05×10^{-3}	tumblr.com	-5.75×10^{-3}	instagram.com	-5.16×10^{-3}
twittascope.com	-1.79×10^{-3}	economist.com	5.54×10^{-3}	foxnews.com	-5.10×10^{-3}
tumblr.com	-1.73×10^{-3}	bloomberg.com	5.01×10^{-3}	msn.com	-4.86×10^{-3}

(B1): Chn(19) + Iran(19) → Rus(18) / Rus(20)

domain	IG(val.)	domain	IG(test)	domain	IG(base.)
nbcnews.com	3.28×10^{-3}	inc.com	-7.94×10^{-3}	nytimes.com	-2.07×10^{-2}
tumblr.com	-2.85×10^{-3}	yahoo.com	-3.76×10^{-3}	abouthub.info	-1.22×10^{-2}
house.gov	-2.78×10^{-3}	nbcnews.com	2.32×10^{-3}	politico.com	-1.09×10^{-2}
senate.gov	2.50×10^{-3}	foursquare.com	-1.88×10^{-3}	conta.cc	-1.08×10^{-2}
pscp.tv	2.41×10^{-3}	soundcloud.com	1.69×10^{-3}	senate.gov	8.49×10^{-3}
foursquare.com	-2.16×10^{-3}	espn.com	-1.34×10^{-3}	abcnews.com	-7.85×10^{-3}
wordpress.com	-2.05×10^{-3}	usatoday.com	-1.16×10^{-3}	reddit.com	-6.85×10^{-3}
thehill.com	-2.01×10^{-3}	washingtonpost.com	-1.15×10^{-3}	mailchimp.com	-6.82×10^{-3}
washingtonpost.com	-1.95×10^{-3}	change.org	1.11×10^{-3}	wsj.com	-6.40×10^{-3}
furnishhome.ru	-1.84×10^{-3}	apnews.com	1.06×10^{-3}	github.com	-6.19×10^{-3}
bbc.co.uk	1.51×10^{-3}	house.gov	-1.05×10^{-3}	wabcradio.com	-6.12×10^{-3}
forbes.com	-1.44×10^{-3}	sba.gov	9.44×10^{-4}	hubs.ly	-5.82×10^{-3}
yahoo.com	-1.41×10^{-3}	senate.gov	9.17×10^{-4}	foxnews.com	-5.82×10^{-3}
bglradio.net	-1.41×10^{-3}	pinterest.com	-8.24×10^{-4}	instagram.com	-5.75×10^{-3}
flwrs.com	-1.36×10^{-3}	huffpost.com	-7.92×10^{-4}	msn.com	-5.26×10^{-3}

(B2): Rus(18) + Iran(19) → Chn(19) / Chn(20)

domain	IG(val.)	domain	IG(test)	domain	IG(base.)
washingtonpost.com	-2.20×10^{-3}	justunfollow.com	6.73×10^{-3}	nytimes.com	-1.85×10^{-2}
cnm.com	-2.02×10^{-3}	tumblr.com	-6.54×10^{-4}	abouthub.info	-1.06×10^{-2}
twittascope.com	-1.56×10^{-3}	etsy.com	-5.16×10^{-4}	conta.cc	-1.04×10^{-2}
wordpress.com	-1.09×10^{-3}	yahoo.com	-5.03×10^{-4}	politico.com	-1.00×10^{-2}
senate.gov	1.04×10^{-3}	cnm.com	-4.89×10^{-4}	senate.gov	8.92×10^{-3}
cdt.org	9.19×10^{-4}	foursquare.com	-4.69×10^{-4}	abcnews.com	-7.24×10^{-3}
yahoo.com	-8.57×10^{-4}	house.gov	-3.58×10^{-4}	reddit.com	-6.16×10^{-3}
sen.gov	-8.55×10^{-4}	conservativejun[*].com	3.32×10^{-4}	wsj.com	-5.92×10^{-3}
theconversation.com	8.21×10^{-4}	medium.com	-2.83×10^{-4}	mailchimp.com	-5.55×10^{-3}
medium.com	-7.94×10^{-4}	theconversation.com	-2.27×10^{-4}	wabcradio.com	-5.50×10^{-3}
epsomguardian.co.uk	7.85×10^{-4}	apnews.com	2.06×10^{-4}	hubs.ly	-5.48×10^{-3}
msn.com	-7.39×10^{-4}	github.com	-1.98×10^{-4}	instagram.com	-5.29×10^{-3}
bloomberg.com	7.12×10^{-4}	wired.com	-1.94×10^{-4}	foxnews.com	-5.28×10^{-3}
furnishhome.ru	-6.89×10^{-4}	sba.gov	1.66×10^{-4}	msn.com	-5.02×10^{-3}
inewssource.org	6.69×10^{-4}	cnsnews.com	-1.49×10^{-4}	github.com	-4.80×10^{-3}

(B3): Chn(19) + Rus(18) → Iran(19) / Iran(21)

domain	IG(val.)	domain	IG(test)	domain	IG(base.)
foursquare.com	-4.15×10^{-3}	gofundme.com	1.80×10^{-2}	nytimes.com	-1.95×10^{-2}
cnm.com	-3.91×10^{-3}	bbc.co.uk	1.28×10^{-2}	conta.cc	-1.12×10^{-2}
house.gov	-3.85×10^{-3}	twittascope.com	-9.93×10^{-3}	abouthub.info	-1.09×10^{-2}
medium.com	-3.66×10^{-3}	house.gov	-9.60×10^{-3}	politico.com	-1.04×10^{-2}
huffpost.com	-3.38×10^{-3}	iheart.com	7.84×10^{-3}	senate.gov	9.25×10^{-3}
senate.gov	2.67×10^{-3}	wordpress.com	-7.82×10^{-3}	abcnews.com	-7.66×10^{-3}
apple.news	-2.44×10^{-3}	npr.org	7.49×10^{-3}	reddit.com	-6.26×10^{-3}
amazon.com	-2.10×10^{-3}	cnm.com	-6.56×10^{-3}	wsj.com	-5.96×10^{-3}
greenlifestylech[*].com	1.84×10^{-3}	washingtonex[*].com	6.13×10^{-3}	github.com	-5.93×10^{-3}
tumblr.com	-1.70×10^{-3}	senate.gov	6.10×10^{-3}	mailchimp.com	-5.86×10^{-3}
usa.gov	-1.63×10^{-3}	justunfollow.com	5.54×10^{-3}	wabcradio.com	-5.82×10^{-3}
economist.com	1.62×10^{-3}	bloomberg.com	5.52×10^{-3}	instagram.com	-5.67×10^{-3}
theguardian.com	-1.51×10^{-3}	tumblr.com	-5.47×10^{-3}	foxnews.com	-5.65×10^{-3}
yahoo.com	-1.46×10^{-3}	wired.com	-5.17×10^{-3}	hubs.ly	-5.40×10^{-3}
conta.cc	-1.37×10^{-3}	economist.com	4.89×10^{-3}	msn.com	-5.10×10^{-3}

Table 5. IG values for individual domains in each trial and val, test, and baseline set. For long domain names, [*] denotes truncation.

E Frequent and Removed domains

Here we show the most frequent domains which are retained or censored in each dataset. We specifically show the result at the most stringent threshold $\gamma_{\max} = 0.4$ where MLP still demonstrates strong performance.

Baseline

indicator	counts	indicator	tf-idf	censored ($\gamma_{\max}=0.4$)	counts
UNCOMMON	770187	instagram.com	1464.24	twitter.com	1571276
instagram.com	283505	house.gov	511.7	youtube.com	211489
twittascope.com	91120	flwrs.com	477.48	facebook.com	106082
house.gov	68485	soundcloud.com	417.33	vine.co	25835
nytimes.com	58666	twittascope.com	415.91	ift.tt	22096
washingtonpost.com	37356	nytimes.com	380.88	google.com	17822
senate.gov	28874	foxnews.com	289.61	blogspot.com	16239
usa.gov	20972	espn.com	288.08	cnn.it	8579
theguardian.com	20216	washingtonpost.com	286.39	reuters.com	8203
huffpost.com	19937	pscp.tv	281.8	bbc.in	8193
wsj.com	19904	github.com	250.51	hill.cm	7066
foxnews.com	19632	www.gov.uk	240.47	fxn.ws	6111
tumblr.com	19555	wordpress.com	239.23	breitbart.com	5917
pinterest.com	19031	apple.com	236.77	chinanews.com	5753
bloomberg.com	18553	twitch.tv	220.57	telegraph.co.uk	5287
foursquare.com	18350	huffpost.com	219.8	twimg.com	5157
wordpress.com	17313	tumblr.com	217.38	vimeo.com	5028
soundcloud.com	17177	birdops.com	210.94	nypost.com	5007
flwrs.com	16862	snpy.tv	210.9	etsy.com	4062
apnews.com	16724	foursquare.com	207.91	dailycaller.com	4038
swarmapp.com	15441	amazon.com	206.87	kp.ru	3865
amazon.com	14282	theguardian.com	196.59	spoti.fi	3850
cnn.com	14275	bbc.co.uk	195.18	independent.co.uk	3839
pscp.tv	13428	atmlb.com	193.08	unfollowspy.com	3734
usatoday.com	12696	gofundme.com	181.99	t.me	3641
politico.com	12322	linkedin.com	175.83	vk.com	3636
thehill.com	12002	uapp.ly	171.29	livejournal.com	3621
medium.com	11073	curiouscat.me	169.83	bbc.com	3406
etsy.com	9797	pinterest.com	166.41	spotify.com	3340
bbc.co.uk	9624	buzzfeed.com	165.26	dailymail.co.uk	3222
npr.org	9299	usa.gov	164.36	newsweek.com	3189
forbes.com	8892	conta.cc	160.76	ruposters.ru	3170
cnbc.com	8800	senate.gov	159.12	rusnovosti.ru	3147
linkedin.com	8664	medium.com	157.13	periodismodeportivo[*].com	3121
apple.com	8524	eventbrite.com	150.9	twitpic.com	3070
github.com	8477	ble.ac	143.32	regnum.ru	2855
ebay.com	8190	wsj.com	143.09	smarturl.it	2812
eventbrite.com	8082	cnn.com	139.38	lat.ms	2597
crowdfireapp.com	8039	hudl.com	133.94	cbsloc.al	2577
untappd.com	8009	politico.com	128.7	rbc.ru	2425
iacr.org	7715	usatoday.com	126.92	dld.bz	2423
yahoo.com	6787	forbes.com	126.03	yfrog.com	2344
latimes.com	6756	iacr.org	122.46	washex.am	2300
conta.cc	6554	crowdfireapp.com	122.11	read.bi	2197
cbsnews.com	6546	thehill.com	121.6	soompi.com	2192
buzzfeed.com	6486	change.org	121.29	chicagotribune.com	2182
apple.news	6427	untappd.com	121.19	washingtontimes.com	2177
www.gov.uk	6349	nfl.com	117.88	theblaze.com	2176
time.com	5862	npr.org	114.22	mash.to	2031
abouthub.info	5761	abcnews.com	114.22	conscores.org	2010
vox.com	5596	apple.news	109.49	miamiherald.com	2002
flipit.com	5560	bible.com	109.38	sfgate.com	1895

Russia (2018)

indicator	counts	indicator	tf-idf	censored ($\gamma_{\max}=0.4$)	counts
UNCOMMON	101869	instagram.com	501.11	livejournal.com	617933
instagram.com	27361	cnn.com	481.74	riafan.ru	452984
washingtonpost.com	16305	wikipedia.org	263.78	twitter.com	285859
foxnews.com	12065	oprf.ru	257.69	ria.ru	166088
nytimes.com	6143	sdelanounas.ru	216.52	yandex.ru	152580
usatoday.com	4831	swarmapp.com	180.14	gazeta.ru	129518
huffpost.com	4520	dni.ru	137.09	youtube.com	122115
theguardian.com	4220	nytimes.com	118.84	rt.com	84782
wordpress.com	3965	rvns.co	108.87	ift.tt	64237
tumblr.com	3242	ukraina.ru	99.21	nevnov.ru	63584
soundcloud.com	3190	tumblr.com	98.1	vesti.ru	52729
politico.com	2769	iz.ru	84.76	kievsmi.net	50567
cnn.com	2529	crowdfireapp.com	57.37	vk.com	45196
apnews.com	2315	theguardian.com	56.06	kiev-news.com	44616
wsj.com	2306	wordpress.com	54.68	inforeactor.ru	39339
rawstory.com	1892	huffpost.com	53.88	championat.com	35713
bloomberg.com	1867	whitehouse.gov	48.24	lenta.ru	34658
thehill.com	1805	apple.com	47.39	tass.ru	33355
pscp.tv	1634	change.org	46.88	emaidan.com.ua	33270
washingtonexaminer.com	1589	snpy.tv	44.71	vine.co	25509
abcnews.com	1563	soundcloud.com	43.95	vk.cc	23394
wikipedia.org	1504	washingtonpost.com	42.22	lifenews.ru	23009
amazon.com	1432	sky.com	40.49	rbc.ru	22143
buzzfeed.com	1391	foxnews.com	39.41	podrobnosti.biz	21969
nbcnews.to	1384	afp.com	39.19	nahnews.com.ua	21049
freebeacon.com	1321	bbc.co.uk	39.09	izvestia.ru	20644
townhall.com	1285	wsj.com	38.62	fontanka.ru	20545
time.com	1264	golos-dnr.ru	35.71	e1.ru	20142
swarmapp.com	1218	amazon.com	32.78	exerciseworkout.pw	17285
yahoo.com	1185	usatoday.com	29.25	mr-7.ru	17228
medium.com	1057	rusnext.ru	27.76	losefattips.pw	16805
apple.com	1009	salon.com	23.24	facebook.com	16364
cbsnews.com	991	espn.com	22.94	breitbart.com	16292
vice.com	979	pscp.tv	22.73	twib.in	16089
latimes.com	882	msn.com	22.29	cbslocal.com	15810
nationalreview.com	830	rawstory.com	21.05	om1.ru	15372
snpy.tv	782	nbcnews.to	20.51	prokazan.ru	14887
dailywire.com	745	vice.com	18.93	inosmi.ru	14757
motherjones.com	679	sumall.com	18.38	msk.ru	14590
npr.org	672	politico.com	18.36	ksnt.com	14572
shareaholic.com	671	buzzfeed.com	18.19	dailym.ai	14435
usa.gov	663	bloomberg.com	18.17	tvrain.ru	14293
sdelanounas.ru	647	time.com	17.77	161.ru	13696
msnbc.com	626	iheart.com	17.55	newsnn.ru	13608
slate.me	608	freebeacon.com	17.09	trkterra.ru	13468
apple.news	604	apnews.com	16.67	meduza.io	13455
bbc.co.uk	593	uapp.ly	16.66	sport-express.ru	13349
redstate.com	589	healthcare.gov	16.47	74.ru	13024
thedailybeast.com	586	businessinsider.com	15.61	burnfat.pw	12865
lifenews.com	575	aka.ms	15.27	exercisepw.pw	12396
twittascope.com	549	economist.com	15.03	newinform.com	12350
cnn.com	541	atmlb.com	14.67	losefat.pw	11831

China (2019)

indicator	counts	indicator	tf-idf	censored ($\gamma_{\max}=0.4$)	counts
UNCOMMON	131091	instagram.com	110.62	twitter.com	526189
instagram.com	17516	forbes.com	101.06	dld.bz	195629
nytimes.com	8756	wsj.com	83.31	youtube.com	137703
tumblr.com	6757	nba.com	74.34	feedburner.com	115155
soundcloud.com	5850	pscp.tv	57.7	miss50percent.de	107453
bbc.co.uk	3153	twitch.tv	49.74	happymuslimfamily.net	62821
uapp.ly	2514	tumblr.com	45.29	ift.tt	52636
wordpress.com	1902	uapp.ly	43.4	blogspot.com	43738
forbes.com	1824	nytimes.com	42.68	tandl.me	43348
etsy.com	1720	curiouscat.me	39.99	telkomsel.com	19472
latimes.com	1598	time.com	39.77	mychinanews.com	19221
pscp.tv	1486	soundcloud.com	34.44	google.com	19212
amazon.com	1205	natgeo.com	34.39	favstar.fm	18991
huffpost.com	1109	apple.com	33.13	tsel.me	18721
espn.com	1044	amazon.com	30.43	iphonehacks.com	18097
twitch.tv	990	app.link	27.99	facebook.com	18028
flwrs.com	906	scmp.com	25.93	hampersbylucy.co.uk	16229
apple.com	878	reddit.com	25.87	entrepreneur.com	15844
wsj.com	848	wordpress.com	23.63	glentretenimento.com	15543
cnn.com	818	amazonaws.com	23.25	bbc.in	12567
crowdfireapp.com	741	bbc.co.uk	22.29	kom.ps	12233
foursquare.com	666	flwrs.com	20.95	tistory.com	11974
tcn.ch	656	foodandwine.com	20.42	rol.co.id	11776
foxnews.com	617	crowdfireapp.com	19.81	curiosidadeinformacao.com	11416
datpiff.com	605	variety.com	18.58	chinanews.com	11414
yahoo.com	569	onlyfans.com	18.12	feedsportal.com	11266
theguardian.com	539	cnn.com	17.64	blingbling.guru	11177
engadget.com	532	yahoo.com	17.48	na-ss.com	10750
curiouscat.me	523	justunfollow.com	17.4	ask.fm	10293
gigam.es	492	ew.com	16.95	twitpic.com	10112
feedly.com	398	pinterest.com	16.09	herokuapp.com	9163
twittascope.com	396	politico.com	15.68	seocheckout.com	9084
washingtonpost.com	383	younow.com	15.43	cgtn.com	9033
typepad.com	379	flickr.com	15.26	okezone.com	8969
swarmapp.com	345	linkfire.com	14.85	noticiasboa.com	8420
justunfollow.com	338	espn.com	14.37	mejorsaludybelleza.com	8304
pinterest.com	328	fiverr.com	14.09	ithome.com	7987
pulse.me	327	etsy.com	13.74	osversos.com	7909
military.com	297	theguardian.com	13.05	nicovideo.jp	7254
mashable.com	290	cbsnews.com	12.99	antonioarzola.net	7057
linkedin.com	287	shareaholic.com	12.79	thingstodoinleicester.com	6607
flickr.com	274	cntraveler.com	12.54	segurosdecochebaratos101.com	6354
nba.com	262	foursquare.com	12.32	top-domains.ch	6167
patch.com	257	facebook.com	12.06	sinaimg.cn	5917
bloomberg.com	246	medium.com	11.75	sina.com.cn	5664
microsoft.com	233	ebay.com	11.33	dleconcepts.com	5513
natgeo.com	226	nbcsports.com	10.98	envoque.news	5374
justgiving.com	224	eonline.com	10.71	apltrak.com	4638
usatoday.com	224	bleacherreport.com	10.7	ecns.cn	4533
usa.gov	212	pagesix.com	10.48	roundteam.co	4498
foodandwine.com	205	theglobeandmail.com	10.46	tmi.me	4495
thinkprogress.org	197	washingtonpost.com	10.44	tuguchis.mx	4384

Iran (2019)

indicator	counts	indicator	tf-idf	censored ($\gamma_{\max}=0.4$)	counts
UNCOMMON	511760	instagram.com	242.26	awdnews.com	332374
instagram.com	13943	theguardian.com	184.91	twitter.com	241386
theguardian.com	2506	pscp.tv	158.72	irib.ir	217793
amazon.com	1980	amazon.com	97.03	parstoday.com	153488
nytimes.com	1977	mirror.co.uk	95.83	tel-aviivtimes.com	143601
wordpress.com	1768	reddit.com	92.89	countdown2040.com	139262
huffpost.com	1602	soundcloud.com	87.84	nilenetonline.com	113892
bbc.co.uk	1368	huffpost.com	75.28	youtube.com	97822
reddit.com	1223	wikipedia.org	73.22	sahartv.ir	68003
pscp.tv	1221	nytimes.com	73.2	ift.tt	61936
washingtonpost.com	1155	wordpress.com	72.01	whatsupic.com	56026
cnn.com	1140	ebay.com	68.85	hugedomains.com	53051
bloomberg.com	1077	bbc.co.uk	67.95	7sabah.com	40922
fllwrs.com	909	cnn.com	57.24	blogspot.com	37202
npr.org	883	change.org	53.08	iuvmpress.com	37175
pinterest.com	863	bloomberg.com	50.72	7sabah.com.tr	36348
ebay.com	826	washingtonpost.com	47.99	facebook.com	31935
soundcloud.com	824	fllwrs.com	47.48	rt.com	30039
cnbc.com	673	pinterest.com	45.27	libertyfrontpress.com	26177
rawstory.com	570	swarmapp.com	44.21	al-hadath24.com	25096
yahoo.com	508	medium.com	43.87	beritadunia.net	24965
mirror.co.uk	483	npr.org	43.29	realnienovosti.com	24529
oregonlive.com	470	oregonlive.com	41.59	hindkhabar.in	23440
politico.com	459	rawstory.com	38.14	sachtimes.com	23102
etsy.com	448	buffer.com	37.78	alwaght.com	18792
usatoday.com	411	altnews.in	37.41	whatthebeep.in	16635
change.org	404	etsy.com	36.85	islamtimes.org	15430
forbes.com	373	yahoo.com	34.42	iuvmonline.com	15004
medium.com	332	wef.ch	33.9	alwasatnews.com	14972
apple.com	327	metro.co.uk	33.5	jordan-times.com	14943
wikipedia.org	326	apnews.com	33.33	hindkhabar.com	12604
wsj.com	324	afp.com	28.55	hourriya-tagheer.org	12354
salon.com	297	ebay.to	26.87	theroot.com	12111
vice.com	296	cnbc.com	25.59	qudspal.com	11930
economist.com	293	sky.com	25.35	documentinterdit.com	11816
ebay.to	263	sumall.com	25.23	nthnews.net	11690
apnews.com	254	politico.com	24.88	ptv.io	11540
tumblr.com	252	cpix.me	24.49	telegram.me	8909
thinkprogress.org	231	theintercept.com	24.15	jamnews.ir	8302
sky.com	231	thehill.com	23.77	yedinot.com	8167
vox.com	228	salon.com	23.67	al-saudia.net	8143
foxnews.com	228	huffingtonpost.co.uk	22.06	alwaienews.net	7902
thehill.com	222	apple.com	21.29	wilayat.in	6908
nbcnews.com	218	google.co.uk	20.12	tahreerparty.net	5955
scientificamerican.com	217	thetimes.co.uk	20.04	reportaseislam.com	5842
time.com	212	ynetnews.com	19.95	alkawthartv.com	5535
cbsnews.com	209	economist.com	19.44	realiran.org	5504
ft.com	208	scientificamerican.com	19.31	toonsonline.net	5195
talkingpointsmemo.com	200	thinkprogress.org	19.15	pakonlinenews.com	5176
go.com	199	go.com	18.68	isna.ir	5084
abcnews.com	195	irishtimes.com	18.54	presstv.ir	4709
businessinsider.com	188	vice.com	18.42	mdn.tv	4638

Russia (2020)

indicator	counts	indicator	tf-idf	censored ($\gamma_{\max}=0.4$)	counts
UNCOMMON	33522	iz.ru	293.69	lenta.ru	213528
instagram.com	22190	dni.ru	193.44	yandex.ru	176599
foursquare.com	7586	instagram.com	144.6	rambler.ru	72433
swarmapp.com	2104	quora.com	126.54	newkaliningrad.ru	62448
furnishhome.ru	1151	thenextweb.com	115.03	161.ru	42756
iz.ru	615	furnishhome.ru	107.5	profile.ru	41755
dni.ru	552	foursquare.com	78.0	ufa1.ru	39093
ft.com	532	change.org	61.06	76.ru	37515
crowdfireapp.com	521	anekdot.ru	57.35	vk.cc	29395
tumblr.com	518	apple.com	30.15	ngs24.ru	28842
nytimes.com	467	diletant.media	29.41	twitter.com	25478
wsj.com	405	tumblr.com	22.09	29.ru	24533
sdelanounas.ru	373	finanz.ru	19.72	ngs55.ru	23252
wordpress.com	365	pscp.tv	18.61	youtube.com	22823
change.org	329	wordpress.com	18.02	ali.pub	18388
sumall.com	252	wikipedia.org	16.82	livejournal.com	17377
theguardian.com	236	buzzfeed.com	15.44	er.ru	15853
linkedin.com	227	medium.com	14.77	dropi.ru	15011
apple.com	206	crowdfireapp.com	14.53	45.ru	10915
medium.com	203	smotrim.ru	14.33	mos.ru	10406
washingtonpost.com	197	sdelanounas.ru	12.61	facebook.com	9954
wikipedia.org	181	forbes.com	10.57	ria.ru	9256
csmonitor.com	173	oprfr.ru	10.12	kinopoisk.ru	9084
izhgpk.ru	169	swarmapp.com	9.91	valdaiclub.com	8720
soundcloud.com	164	strana.ua	9.71	life.ru	6978
forbes.com	155	flickr.com	9.3	filmz.ru	5855
flwrs.com	149	elle.com	8.54	vk.com	5114
newsomsk.ru	134	linkfire.com	8.28	tass.ru	5108
huffpost.com	122	ukraina.ru	7.66	mail.ru	5054
gizmodo.com	101	ustream.tv	7.21	gazeta.ru	4298
thenextweb.com	88	bbc.co.uk	7.02	t.me	3579
nike.com	87	nasa.gov	6.94	auto.ru	3413
awe.sm	74	brave.com	6.71	rt.com	3384
bloomberg.com	72	natgeo.com	6.7	onedio.ru	3357
bbc.co.uk	71	reddit.com	6.33	onf.ru	2539
pscp.tv	71	awe.sm	6.27	orientalreview.org	2443
cnn.com	56	izhgpk.ru	5.15	openreporter.ru	2347
thinkprogress.org	54	socialmediatoday.com	5.12	kp.ru	2287
ustream.tv	53	gotowebinar.com	4.96	championat.com	2230
anekdot.ru	52	military.com	4.57	twitpic.com	2210
time.com	51	flipit.com	4.54	regnum.ru	2136
diletant.media	45	tcn.ch	4.47	ridus.ru	2120
thediplomat.com	42	rollingstone.com	4.38	sports.ru	2081
foreignpolicy.com	41	nytimes.com	4.37	antimaidan.ru	2081
motherjones.com	40	esquire.com	4.19	n1.ru	2080
whitehouse.gov	39	nike.com	4.08	rbc.ru	1973
valuemytweets.com	36	shareaholic.com	3.73	interfax.ru	1968
oprfr.ru	36	slideshare.net	3.68	lifenews.ru	1947
buzzfeed.com	35	whitehouse.gov	3.64	ihodl.com	1945
theverge.com	35	facebook.com	3.6	izvestia.ru	1860
quora.com	34	wsj.com	3.56	bbratstvo.com	1840
thehill.com	33	sumall.com	3.48	uwidata.com	1705

China (2020)

indicator	counts	indicator	tf-idf	censored ($\gamma_{\max}=0.4$)	counts
UNCOMMON	1693	axios.com	164.41	youtube.com	8148
axios.com	231	linkfire.com	29.84	twitter.com	1130
medium.com	36	adobe.com	14.58	creaders.net	829
pscp.tv	31	bloomberg.com	13.46	temaretik.com	669
bloomberg.com	30	wordpress.com	10.48	rapradar.com	503
cnn.com	26	weebly.com	10.32	pansci.asia	348
nytimes.com	24	medium.com	10.03	dwnews.com	263
amazon.com	21	amazon.com	9.86	russian7.ru	262
foxnews.com	18	pscp.tv	9.31	creu.ru	249
linkfire.com	17	people.com	6.79	femmie.ru	248
instagram.com	13	fiverr.com	6.69	yandex.ru	235
theguardian.com	10	onlyfans.com	6.6	temadnya.com	188
washingtonpost.com	10	diletant.media	6.2	mychinanews.com	184
cbsnews.com	10	change.org	5.69	facebook.com	149
weebly.com	9	app.link	5.51	cyrillitsa.ru	146
wordpress.com	9	apple.com	5.43	russian7.ru	140
nu.nl	9	yahoo.com	5.35	back-in-ussr.com	138
time.com	9	nike.com	5.27	bbc.com	131
usatoday.com	9	nytimes.com	5.2	chinanews.com	122
lasvegassun.com	7	wsj.com	4.07	vseonauke.com	112
yahoo.com	7	bbc.co.uk	4.06	lifelacker.ru	107
wsj.com	6	cc.com	4.04	kulturologia.ru	102
apple.com	5	washingtonpost.com	3.96	targetplay.ru	101
economist.com	5	standard.co.uk	3.81	dnpmag.com	99
app.link	5	swarmapp.com	3.67	cgtn.com	97
bbc.co.uk	5	buzzfeednews.com	3.66	interesnosti.com	92
swarmapp.com	4	viewbug.com	3.42	p2pb2b.io	90
change.org	4	fanlink.to	3.27	discuss.com.hk	85
katu.com	4	time.com	3.08	pics.ru	79
rfa.org	4	instagram.com	3.03	novate.ru	79
broadway.com	4	anchor.fm	2.91	mistika.xyz	77
natgeo.com	3	tumblr.com	2.88	sci-hit.com	70
tumblr.com	3	natgeo.com	2.86	greatpicture.ru	66
adobe.com	3	theguardian.com	2.36	blogspot.com	64
quora.com	3	uscis.gov	2.35	grammy-s.ru	59
google.com	3	pandora.com	2.28	trendymen.ru	58
insider.com	3	cnn.com	2.1	omode.info	51
soundcloud.com	3	justice.gov	2.06	ift.tt	51
variety.com	3	foxnews.com	2.03	bet535casinoonline.com	49
nikkei.com	2	cnet.com	1.94	kzg.io	47
diletant.media	2	lasvegassun.com	1.82	snatchnews.com	46
wistia.com	2	soundcloud.com	1.81	disq.us	45
obama.org	2	variety.com	1.62	globaltimes.cn	44
mediamatters.org	2	pbs.org	1.47	bonus.express	40
meet Edgar.com	2	eonline.com	1.32	klikabol.com	40
marvel.com	2	foreignpolicy.com	1.25	cluber.com.ua	38
sns.mx	2	cbsnews.com	1.2	everve.net	38
people.com	2	apnews.com	1.12	mirvokrugnas.com	37
petapixel.com	2	quora.com	1.02	adme.ru	35
eonline.com	2	usatoday.com	0.81	tothemoon.game	34
forbes.com	2	economist.com	0.59	promoidom.com	33
fiverr.com	2	etsy.com	0.49	medpravila.com	32

Iran (2021)

indicator	counts	indicator	tf-idf	censored ($\gamma_{\max}=0.4$)	counts
UNCOMMON	1338	nytimes.com	19.49	htv.mx	98259
nytimes.com	373	wsj.com	18.16	hispan.tv.com	43193
cbsnews.com	213	instagram.com	10.53	youtube.com	35874
theguardian.com	208	theguardian.com	9.81	twitter.com	4918
wsj.com	203	rawstory.com	9.2	hispan.tv.ir	1312
washingtonpost.com	186	whitehouse.gov	7.52	bing.com	451
cnn.com	186	pscp.tv	7.21	facebook.com	430
instagram.com	171	cnn.com	6.01	beritadunia.net	344
rawstory.com	148	usatoday.com	5.79	thatsmags.com	334
pscp.tv	111	washingtonpost.com	5.07	cnn.it	288
thehill.com	97	forbes.com	4.12	bc.game	284
politico.com	76	thehill.com	4.07	thealtworld.com	272
businessinsider.com	69	dailywire.com	3.98	balkanspost.com	263
huffpost.com	64	theverge.com	3.62	ahtribune.com	203
foxnews.com	59	flipit.com	3.61	peek.link	180
nbcnews.com	55	msn.com	3.44	tiredearth.com	161
usatoday.com	53	theconversation.com	3.25	kitco.com	152
thedailybeast.com	52	latimes.com	3.18	cryptoglobe.com	144
msn.com	45	businessinsider.com	3.15	cointelegraph.com	125
forbes.com	44	mediaite.com	3.1	bbc.com	103
economist.com	39	politico.com	3.02	reuters.com	102
time.com	35	change.org	2.98	hispan.tv.net	99
yahoo.com	33	abcnews.com	2.89	newsweek.com	89
grahamchuley.com	31	nbcnews.com	2.82	caitlinjohnstone.com	89
abcnews.com	30	cbsnews.com	2.8	independent.co.uk	86
npr.org	28	wordpress.com	2.76	hill.cm	84
vox.com	27	sfchronicle.com	2.63	liputan6.com	78
cnbc.com	26	thepetitionsite.com	2.38	paulcraigroberts.org	78
axios.com	26	soundcloud.com	2.19	farsnews.ir	76
clevelandclinic.com	26	theweek.com	2.06	blabber.buzz	73
apnews.com	26	amazon.com	2.0	whatsapp.com	59
msnbc.com	24	sky.com	1.91	detik.com	54
latimes.com	23	substack.com	1.9	nu.or.id	50
hillreporter.com	23	variety.com	1.9	digitalfinancenews.com	49
slate.com	22	oregonlive.com	1.89	aljazeera.com	49
change.org	21	axios.com	1.87	rt.com	43
bloomberg.com	20	thedailybeast.com	1.85	google.com	42
theatlantic.com	20	realclearpolitics.com	1.82	oal.lu	41
medium.com	18	huffpost.com	1.82	ift.tt	41
salon.com	18	theatlantic.com	1.69	sindonews.com	40
mediaite.com	17	time.com	1.58	altcoinss.com	40
motherjones.com	16	apnews.com	1.57	t.me	40
dailykos.com	16	foxnews.com	1.54	politicususa.com	40
theweek.com	15	go.com	1.5	haaretz.com	40
thenationalpulse.com	15	yahoo.com	1.4	tradermeetscoder.com	39
petrescuereport.com	14	cnbc.com	1.39	bracingviews.com	39
whitehouse.gov	13	moveon.org	1.09	hrw.org	39
sky.com	13	ca.gov	1.08	dailymail.co.uk	35
go.com	12	vox.com	1.08	fair.org	34
actblue.com	12	msnbc.com	1.08	daysofpalestine.com	30
ft.com	12	medium.com	1.07	theblaze.com	27
newyorker.com	11	salon.com	1.05	ibtimes.com	27